REACTION AND SURFACE CHARACTERIZATION STUDIES OF K- AND Cs-PROMOTED, Zn/Cr SPINEL, HIGHER ALCOHOL SYNTHESIS CATALYSTS

By

WILLIAM S. EPLING

A DISSERTATION PRESENTED TO THE GRADUATE SCHOOL
OF THE UNIVERSITY OF FLORIDA IN PARTIAL FULFILLMENT
OF THE REQUIREMENTS FOR THE DEGREE OF
DOCTOR OF PHILOSOPHY

UNIVERSITY OF FLORIDA

1997

ACKNOWLEDGMENTS

I would like to thank Gar Hoflund for his guidance and assistance during my studies at the University of Florida and my stay in Gainesville. His introduction to life beyond chemical engineering has been inspiring. I would also like to thank Charles Mount and John Wolan for their patience with me in the lab. Furthermore, I must acknowledge B. and B. for their humor and sanity. Finally, I would like to recognize and thank the people most special in my life, my parents and sister, for their support although they did not understand why I chose to stay in school. And to Tonya Klein for her patience, support and understanding from 536 miles away, I extend my deepest appreciation.

TABLE OF CONTENTS

page

ACKNOWLEDGMENTS ii

ABSTRACT iv

CHAPTERS

1 INTRODUCTION 1

Overview 1
Literature Review 4
Fischer-Tropsch Type Catalysts 5
Modified Low-Temperature Methanol Synthesis Catalysts 8
Modified High-Temperature Methanol Synthesis Catalysts 11

2 STUDY OF A K-PROMOTED COMMERCIAL Zn/Cr SPINEL FOR HAS 13

Experimental 13
Reaction Studies 13
Characterization Studies 14
Results and Discussion 15
Reaction Studies 15
Characterization Studies 17
Summary 22

3 STUDY OF A Cs-PROMOTED COMMERCIAL Zn/Cr SPINEL FOR HAS 35

Experimental 35
Results and Discussion 35
Reaction Studies 35
Characterization Studies 37
Summary 42

4 STUDY OF A K-PROMOTED ZnO CATALYST FOR HAS 55

Experimental 55
Results and Discussion 55
Reaction Studies 55
Characterization Studies 58
Summary 62

REFERENCES 73

BIOGRAPHICAL SKETCH 77

Abstract of Dissertation Presented to the Graduate School
of the University of Florida in Partial Fulfillment of the
Requirements for the Degree of Doctor of Philosophy

REACTION AND SURFACE CHARACTERIZATION STUDIES OF K- AND Cs-PROMOTED, Zn/Cr SPINEL, HIGHER ALCOHOL SYNTHESIS CATALYSTS

By

William S. Epling

August, 1997

Chairman: Gar B. Hoflund
Major Department: Chemical Engineering

An equimolar mixture of methanol and isobutanol produced from syngas would be ideal for downstream production of methyl tertiary-butyl ether (MTBE), an oxygenated additive used in gasoline today. Currently, MTBE is produced from petroleum feedstock and in an effort to reduce this dependence many studies have investigated the use of modified methanol synthesis catalysts to produce mixtures of isobutanol and methanol from coal-derived syngas. Furthermore, the proper mixtures of methanol and higher alcohols can be used directly as fuel in modified internal combustion engines or as an additive (e.g., gasohol). Unfortunately, the catalysts which have been discovered and tested thus far produce high levels of methanol relative to isobutanol with 3-to-1 mole ratios being typical. The production rate of isobutanol is also relatively small to be commercially attractive. In the present series of studies the investigation of Cs and K-promoted Zn/Cr spinel catalysts has led to improvements in product stream compositions. The effects of promotor loading were monitored as well as four sets of reactor conditions in order to optimize the isobutanol production rate. Product flow rates of isobutanol greater than 100 g/kg-hr and methanol-to-isobutanol mole ratios below 1.0

have been attained. Surface characterization studies using X-ray photoelectron spectroscopy (XPS) and ion scattering spectroscopy reveal that the catalyst undergoes changes during the reductive pretreatment and with time on stream in the reactor. These changes can be qualitatively correlated to the catalytic performance. Furthermore, the XPS data consistently indicate that the only phase of Zn in the near-surface region of all the samples examined is ZnO. Therefore, K-promoted ZnO was also tested for higher alcohol synthesis (HAS). Although this catalyst yielded a smaller amount of isobutanol in comparison to the promoted Zn/Cr spinel catalysts on a weight basis, on a surface-area basis this catalyst proves to be superior. Based on these results it has been determined that an alkali-promoted ZnO material is a catalytically active phase in HAS catalysts.

CHAPTER 1
INTRODUCTION

Overview

Gasoline is currently the primary transportation fuel used in the world. The high consumption of fuel and the diminishing supply of domestic oil reserves and oil beds make it necessary to focus attention on improving the efficiency of fuel use and on the use of alternative sources for fuel which are in more abundant supply. Furthermore, growing concerns over the environment have stimulated interest in the use of fuels which result in lower emissions. The interest in pollution control in transportation is due to the fact that the largest source of hydrocarbon emissions in the U.S. is automobile exhaust. Emitted hydrocarbons in the presence of sunlight undergo a series of reactions which create ground-level ozone, the primary ingredient of smog. Emissions containing CO and NO_x from combustion engines are also pollution problems. During the recent past, laws have been implemented which have required a reduction in toxic emissions, and higher fuel qualities and improved catalytic converters provided this change. Throughout the automobile and fuel industries, however, there is a constant effort to make further improvements on fuel quality and more complete combustion of the fuel.

Alcohols and ethers as fuels can provide solutions for these problems. Most ethers and alcohols have high octane ratings and burn to produce primarily water and carbon dioxide. These oxygenates can be used directly as transportation fuels; however, extensive modification of engines, fuel delivery systems and national and global distribution facilities would be necessary and quite costly. Most likely, the use of the oxygenates as fuels will not occur in the near future unless environmental legislation forces the issue. Alcohols and ethers, however, also can be added to gasoline in quantities of 10 to 20% without having to adapt vehicle engines. In this capacity, no

changes are necessary in the distribution facilities and the volume of gasoline consumption is reduced. Alcohol mixtures blended with gasoline and ether additives in gasoline both are used currently in the U.S. fuel market. Methyl tertiary-butyl ether (MTBE) is found in most of the unleaded gasoline today. Ethers, particularly MTBE will continue to be used as additives in the future and their role is expected to increase. Furthermore, the use of these additives has beneficial effects beyond reducing the consumption of fuel through displacement by the additive. For example, MTBE is soluble in gasoline, requiring no cosolvents, acts as an octane enhancer promoting more complete combustion and thus causes a reduction in emissions and can be added up to as much as 15% in gasoline. The t-butyl fragment of the additive is derived from isobutylene which is currently produced from petroleum. The production of MTBE from this reaction pathway can therefore be limited by the C_4 petroleum feedstock availability.

Gasoline blends containing anhydrous fermentation ethanol (gasohol) also are used as motor fuels today. These mixtures have an acceptable water tolerance, an excellent octane quality and acceptable volatility and materials compatibility. Although ethanol performs well as a gasoline extender, the production of fermentation ethanol is not viable from an economic standpoint. Government exemptions or assistance are necessary to make this process industrially competitive. Methanol-gasoline blends can also be used as a fuel source for vehicles, but the mixture requires the presence of a higher alcohol in order to achieve acceptable volatilities and water tolerance levels. The performance of these blends is quite dependent on the concentration of the methanol in the blend as well as the ratio of methanol to higher alcohol used.

An alternative route in the production of MTBE from petroleum feedstock or in the production of alcohol mixtures would use a domestically abundant source of fuel, namely coal. Coal-derived fuels can be produced through two methods. The direct liquefaction method involves the high pressure hydrogenation of coal to liquid hydrocarbons. The indirect liquefaction method converts the coal to syngas, a mixture of

CO and H_2, which may then be upgraded to motor fuels or fuel additives. One such indirect process is the Fischer-Tropsch process. In this process CO and H_2 are reacted over catalysts to produce hydrocarbons which may be reacted further to form fuel. A broad range of products are produced, however, and careful downstream separation processes are required. The heavier products of this reaction process, such as waxes, must be cracked to be useful and also may stick to and therefore destroy the catalyst. Another inefficiency is the formation of lighter products as gases which are not useful as transportation fuels. This process has been investigated heavily for over 60 years and more major advancements in the technology are not probable. Another possible approach using coal as an indirect fuel source is an alternative route to form fuel additives such as MTBE or alcohol mixtures using coal-derived syngas. An economically viable pathway which uses syngas to produce the appropriate amounts and ratios of methanol and isobutanol could accomplish this task. For the production of MBTE a separate intermediate process involving the dehydration of the isobutanol to isobutylene would then allow these products to be converted to the fuel additive through known downstream reaction processes. The reactant, syngas, can be produced readily from the abundant domestic supply of coal, thus reducing the dependence on a diminishing domestic petroleum feedstock to produce the additive or appropriate alcohol mixture.

A process designed for higher alcohol synthesis (HAS) could provide the necessary products for downstream synthesis to MTBE or the proper mixtures for use in alcohol-gasoline blends. Higher alcohols, in the C_3 to C_5 range, can be used to provide volatility control and water tolerance in methanol-gasoline blends and a proper mixture of isobutanol and methanol could be used to produce MTBE. An ideal design for these processes would use a low H_2/CO ratio syngas and produce a 1:1 stoichiometric mixture of methanol and isobutanol for downstream MTBE synthesis or a 5.4:1 mixture for direct use as the alcohol mixture fuel additive. A well-designed catalytic reactor process is necessary to achieve this goal and the selectivities and product flow rates must

necessarily be high. Extensive research in developing a catalyst which would provide the desired product stream has been accomplished, and previous work by other groups is discussed below. This study focuses on a series of catalysts which have been developed for HAS to produce the proper product stream for MTBE production. Surface science studies were employed as well to help in the understanding of the catalyst surfaces and ultimately lead to further catalyst improvements. These experiments have led to the development of catalysts which ae superior to those present in the literature examined and lead to a solid basis for attaining a process which would be economically viable in either the production of MTBE or alcohol additives in transportation fuels.

Literature Review

Higher alcohol synthesis from syngas (CO/H_2) has been studied for many years. The possibilities of forming hydrocarbons for fuel, alcohols for direct use as fuel and alcohols as precursors for fuel or fuel additives have been the motivating factors behind the investigations. Some of the earliest studies were performed in order to elucidate the reaction pathway in HAS. Frolich and Cryder (1) in 1930 reported the formation of alcohols higher than methanol by passing syngas over a Zn:Mn:Cr, 1:1.1:1.03, catalyst. It was reported that methanol forms from a formaldehyde intermediate and that the higher alcohols form from the methanol through stepwise condensation reactions. One year later, a study presented by Graves (2) supported this reaction sequence. Since these early studies, three primary groups of catalysts have been adapted and tested for HAS. Modifications in Fischer-Tropsch (FT) type catalysts and in both low-temperature, low-pressure and high-temperature, high-pressure methanol synthesis catalysts result in the conversion of CO and H_2 mixtures to alcohols.

Fischer-Tropsch Type Catalysts

Fischer and coworkers investigated the production of hydrocarbon fuels from syngas beginning in the 1920s and developed iron and cobalt based catalysts for this operation. In later studies by Anderson et al. (3,4), alkali promoted or nitrided FT catalysts were used for HAS. Studies have shown that through temperature and contact time variations the hydrocarbon production can be reduced in favor of alcohol formation over Fe- and Co-containing FT catalysts. Specifically, decreases in operating temperatures and reactant stream contact time increases the alcohol selectivity with ethanol being the primary product (5-7). The modification of Co-containing FT catalysts through Re and Sr promotion for HAS has been studied also (8). These doubly promoted Co catalysts produce C_2 oxygenates, primarily ethanol. The addition of Re promotes the activity while Sr improves the selectivity of the catalyst. The total product distribution, however, follows an Anderson-Schulz-Flory (ASF) distribution. This product distribution is characteristic of the linear condensation polymerization mechanism. A variety of products were therefore observed, and large hydrocarbon productions were noted as well.

The use of Mo containing catalysts have been examined in HAS. Fujimoto and Oba (9) studied a Co-Mo catalyst which was promoted with potassium carbonate. Again the alcohol and the hydrocarbon product stream compositions follow an ASF distribution. The presence of the potassium carbonate is effective in increasing the selectivity to alcohol production through the reduction in hydrocarbon formation. It was also demonstrated that the Co must be in a reduced form for alcohol synthesis. Kiennemann et al. (10) studied the effects of Mo addition to modified iron-based catalysts on HAS. They reported that coprecipitated Fe-Cu-Mo catalysts produce higher linear alcohols and the activities and the selectivities to alcohol formation of these catalysts is greater than those made by the more direct impregnation of a silica support. The alcohol chain growth follows an ASF product distribution. The authors concluded that the rate of

alcohol chain growth is too low in comparison to other types of HAS catalysts, and furthermore, these catalysts are highly sensitive to temperature changes. The synthesis of higher alcohols over Ru-Mo catalysts demonstrate that a synergistic effect between Ru and Mo exists which is necessary for the production of alcohols (11). Promotion of the Al_2O_3 supported Ru-Mo with Na_2O decreases the catalytic activity but increases the selectivity possibly through Ru particle aggregation. Molybdenum supported on SiO_2 catalysts prepared by metal-oxide vapor synthesis (MOVS) have been tested also (12). Higher linear alcohols are produced but in relatively small amounts in comparison to the primary product, methanol. Furthermore, substantial amounts of hydrocarbon byproducts form. The addition of small amounts of Ni, Cs and K to those catalysts does result in better performance than the nonpromoted samples but not to a large degree. Alkali-promoted molybdenum disulfide catalysts have been tested for HAS and the product stream is again limited by an ASF distribution (13). These catalysts require a balance of both the alkali and Mo to achieve maximum alcohol yields which are composed primarily of methanol (14). Other promoted Ni containing catalysts were examined for HAS by Pereira et al. (15). The addition of Li to silica-supported Ni results in higher alcohol formation while Cu addition does not. The addition of Cu, however, increases the stability of the Ni/SiO_2 sample toward CO conversion through the inhibition of subcarbonyl formation however, the CO is not converted to alcohols. The presence of Li adds stability to the subcarbonyl species which causes activity decay due to accumulation of this species. Again, a substantial amount of methanol is produced using the Ni/SiO_2 catalyst, but very small amounts of higher alcohols are. Uchiyama et al. (16) demonstrated that coprecipitated $NiO-TiO_2$ catalysts promoted with Na and Cu can attain good selectivities for HAS, although the primary higher alcohol component of the product stream is ethanol. Further studies using Mo, group VIII metals and alkali catalyst systems have been investigated (9,11,17,18). It was observed that the Mo is necessary

for activity, an ASF product distribution results and a substantial amount of CO_2 is produced when using the Mo-containing catalysts.

The addition of copper to cobalt catalyst systems has also been investigated for HAS. Under the reaction conditions a Cu-Co alloy forms and may be the active site in alcohol formation (19,20). The suppression of hydrocarbon formation can be achieved using these catalysts under extremely careful catalyst preparations. Selectivities of 80% alcohol can be attained and high amounts of ethanol as well. Larger alcohols, however, are produced in smaller amounts. The insertion of CO into an adsorbed alkyl intermediate and metal bond and subsequent dehydrogenation is thought to play a key role in the reaction mechanism (21,22). Unfortunately, these catalysts seem to be susceptible to rapid decay which is possibly due to coke formation at the catalyst surface. Adsorbed hydrocarbons (23) and water have also been observed on the spent catalysts as well as deterioration of the support material. These changes were shown to be irreversible, leading to a constant decay in catalytic activity with time (21). The use of promoted Rh-based catalysts results in HAS as well. Both Rh/ThO_2 and Rh/TiO_2 catalysts, under the appropriate reaction conditions, lead to higher alcohol formation (24,25). The primary alcohol product is ethanol synthesized through a mechanism which is not completely understood but seems to involve the insertion of CO into a Rh-C type bond. A further increase in the formation of ethanol occurs upon ceria promotion of the catalysts (26,27). This promoted effect is attributed to CO bonding through both the C and O at the metal-support interface. Ichikawa and coworkers have observed that the use of promoted Rh catalysts supported on rare-earth oxides are also effective in HAS (27,28). The use of Mn, Ti, Zr and Fe promotors were also particularly effective in increasing the selectivity to oxygenates. These results have been observed by other groups as well (29,30). Bond et al. (31) observed that La_2O_3 promotion of Rh/TiO_2 catalysts enhances the selectivity of oxygenate production and a prolonged induction period was necessary to achieve maximum alcohol yields. Unfortunately, all of the

aforementioned catalysts result in an alcohol product distribution which closely fits an ASF pattern which limits the possibility of isolating certain alcohol chain lengths or attaining high concentrations of a higher alcohol product of one specific length. Methanol and ethanol can be produced in larger amounts, however, isobutanol, the desired product for downstream MTBE synthesis, is formed in much smaller concentrations. This drawback results in the necessity of careful downstream separation processes and a large amount of byproduct alcohols of various chain lengths. Furthermore, these catalysts were designed originally for hydrocarbon synthesis and unfortunately the modifications to these samples do not eliminate the hydrocarbon byproduct formation.

Modified Low-Temperature Methanol Synthesis Catalysts

Lewis and Frolich in 1928 (32) demonstrated that passing a syngas feedstream over a $CuO/ZnO/Al_2O_3$ catalyst results in high methanol yields. Since this discovery, this catalyst type has been adapted for HAS use. Infrared (IR) spectroscopy studies performed by Edwards and Schrader (33,34) show that adsorbed methoxy and formaldehyde species as well as a bidentate formate were present on the catalyst during the reaction process. As in the Cu-containing FT catalysts, the Cu is in a partially reduced state. Promoting these low-temperature, low-pressure, Cu-based methanol synthesis catalysts with alkali results in HAS. Primary alcohols, including methanol, are the main products formed. Vedage et al. (35) investigated the promotion of a Cu/ZnO catalyst with Cs, Rb, K, Na and Li. The better performance in methanol production with the different alkali promotors were found to be in the order just listed, under the reaction conditions examined. A BaOH promotor also was tested but agglomerates on the surface and shows little effect on the catalytic activity when compared to the nonpromoted sample. The alkali hydroxide promotors mentioned above, however, are highly dispersed over the catalyst surfaces. Increasing the reaction temperature above 280°C and lowering

the H_2/CO feed ratio promotes the synthesis of higher alcohols over each of the catalysts which were tested. Nunan and coworkers (36) further investigated the effects of Cs addition to a Cu/ZnO catalyst on the product stream in alcohol synthesis. They reported that the formation of methanol is enhanced upon the addition of Cs under the appropriate conditions. The data presented also indicates that the selectivity toward higher oxygenate synthesis also increases slightly with alkali promotion. A Cs concentration of 0.8 wt.% results in the highest methanol product yield under the experimental conditions used. Further investigations followed which focused on HAS upon Cs addition. Nunan et al. (37) demonstrated that the synthesis rate of ethanol could be significantly enhanced using cesium formate as a promotor. The selectivities of the ethanol or methanol could be changed through modifications of the reaction temperature and syngas ratio, much as Vedage et al. showed (35). Studies were also performed using the Cs-promoted catalysts in which reaction conditions were employed which resulted in HAS, i.e., higher temperatures. A maximum in product yield with Cs loading was obtained between 0.3 and 0.5 wt.% while larger additions of Cs result in smaller surface Cs concentrations and therefore lower yields (38,39). This study also demonstrated that the use of an alumina support decreased the selectivity toward higher alcohol production with time on stream due to a decrease in the Cs concentration at the surface. The use of chromia as a support material leads to the formation of dimethyl ether complexes at the catalyst surface and therefore an undesirable alcohol product distribution. The addition of Cs to the Cr-supported catalysts, however, negates the effect of the chromia resulting in greater alcohol formation. The greatest effect of the Cs on the product stream composition was the $C_2 \rightarrow C_3$ formation which suggests that the presence of Cs increases the rate of ethanol conversion to higher alcohols. A separate study also noted that the selectivity toward HAS increases with Cs addition as well as increased methanol productivity over a $Cu/ZnO/Cr_2O_3$ catalyst (40). Surface science experiments revealed that the Cs presence inhibits the reduction of Cu although after introduction of the reactant syngas stream,

reduced phases are observed. X-ray photoelectron spectroscopy (XPS) and X-ray diffraction (XRD) data indicate that the Zn phase never changes from ZnO. Furthermore, increasing calcination temperatures result in greater activity toward alcohol production possibly due to a surface enrichment of Cs. Even with the addition of Cs, however, these catalysts produce small amounts of alcohols larger than ethanol and typically produce primarily methanol (13,35,38,41). A further disadvantage of these catalyst systems is more hydrocarbon byproduct formation occurs upon comparison to the Cu/ZnO catalysts which contain no Cr.

Smith and Anderson (42) investigated the effects of the addition of K_2CO_3 to a commercial $Cu/ZnO/Al_2O_3$ catalyst as well as variations of the H_2 to CO ratio on the product stream composition. The most ideal reactor conditions result in an alcohol product stream containing 13.7 wt.% isobutanol, but 61.3 wt.% methanol. An optimum promotor concentration of 0.5 wt.% is observed and decreasing the H_2:CO ratio from 2.0 to 0.5 enhances the selectivity of isobutanol formation. The operating temperature of this catalyst reactor bed has a limited range due to low alcohol yields and catalyst instability. Boz et al. (43) examined the use of K-promoted $Cu/ZnO/Al_2O_3$ catalysts for HAS from syngas as well. An optimum K amount of 0.5 wt.% also is observed and higher isobutanol yields are also attained at higher temperatures. A low CO_2 concentration (2%) was found to be favorable for isobutanol production over this catalyst under the conditions used while higher K loadings and CO_2 amounts result in an increase in methanol formation. Certain results indicate that the CO_2 may be incorporated into the higher alcohols if Cu catalytic sites are available (44) and a kinetic model has been developed based on these results (45). The XPS data obtained indicate that isobutanol synthesis is favored by a higher Cu^0/Cu^{+1} ratio and a larger amount of Cu oxidation results in greater methanol synthesis. An initial decay in catalyst activity occurs and is attributed to a decrease in catalyst surface area and a decrease in the Cu/Zn ratio (43). Stiles et al. (46) studied a K-promoted Cu/Mn/Cr catalyst and observed that slight

variations in the reactor operating conditions or catalyst composition result in large variations in the product stream composition indicating certain conditions will result in the desired output in many instances. Under the idealized conditions tested, however, isobutanol made up only 20.2% of the product stream in the best scenario. Further models have been developed which predict the product distributions of higher alcohols or oxygenates over $Cu/ZnO/Al_2O_3$ catalysts with reasonable accuracy (47,48) although none are definite.

Modified High-Temperature Methanol Synthesis Catalysts

The addition of alkali promotors to Mn/Cr/O, Zn/Cr/O and Zn/Mn/Cr/O catalyst systems also can result in HAS from a syngas feedstream. Frolich and Cryder (1) investigated a K-promoted Zn/Mn/Cr catalyst in 1930 which converted syngas to methanol and higher alcohols. Forzatti and coworkers (49) further examined this same catalyst using surface characterization techniques. The data indicate that the as-prepared catalyst sample is composed of a core consisting of a Zn/Cr spinel (49-51) and zinc carbonate. They further postulate that this core is encapsulated by a K_2CrO_4 phase or possibly $KHCO_3$. A Zn/Cr spinel phase is initially observable but is transformed into a ZnO phase upon being activated at 400°C in H_2 but remained in spinel form if reduced at 400°C in N_2. It is possible that the spinel structure is preserved after reduction depending on the catalyst used. This assertion is based on findings which show the spinel structure is unaffected by an H_2 treatment at 400°C using a catalyst prepared in a different study (52). Kiem and Falter (53) have investigated a Zn/Mn system which includes Zr, Li and Pd as well. Using a catalyst consisting of 30.5 wt.% Zr, 15.4 wt.% Mn, 8.6 wt.% Zn, 0.2 wt.% Pd and 1.5 wt.% Li, they were able to obtain a product stream containing 59% isobutanol (740 g/L cat/hr) and 12% methanol. Furthermore, very little hydrocarbon byproduct presence was reported which is probably due to the absence of chromium in the catalyst samples. It is difficult to compare these results with other literature values

due to the higher temperatures, unit variations (g/L cat/hr) used and a poor reactor design description (the amount or catalyst density was not described). Forzatti and coworkers (13), however, claim similar results can be obtained using a Cs-promoted ZnCrO catalyst under the appropriate reaction conditions, and it is mentioned that less hydrocarbon byproduct formation may be achieved using a chromium-free sample. A study in which the Zn/Cr ratio was varied from 0.064 to 1.913 demonstrates that complete conversion of methanol to hydrocarbons can be attained if the sample containing the least amount of zinc, i.e., the highest amount of Cr, is used (54). Thermodynamic investigations (13,55) and kinetic modeling (56,57) have been employed in order to determine the reaction mechanism involved in HAS over these catalysts. These studies demonstrate that the reaction series occurring over the catalyst surface is quite complex and is not easily understood. The use of these catalysts does represent an improvement in the selectivity toward the synthesis of isobutanol (13). The isobutanol-to-methanol ratios are consistently higher using the alkali-modified high-temperature, high-pressure methanol synthesis catalysts. The total product rate of alcohols in the product stream, however, is lower than that of the Cu-containing samples. A previous study (41) therefore used the two catalysts in series to achieve a final product stream which contained larger amounts of isobutanol.

In general, the previous literature has exposed the limitations of the main three catalyst types used in HAS. Using the modified FT catalysts results in a product stream which can be modeled by an ASF scheme. This eliminates the possibility of isolating a specific alcohol chain lengths without careful downstream separation. Modified low-temperature, methanol synthesis catalysts can yield high conversions of alcohols from syngas but with poor selectivity. The use of modified high-temperature methanol synthesis catalysts on the other hand results in good selectivities, but low conversions which is why the two catalysts in series yield better results.

CHAPTER 2
STUDY OF A K-PROMOTED COMMERCIAL Zn/Cr SPINEL FOR HAS

The present chapter focuses on the optimization of isobutanol synthesis and the methanol-to-isobutanol ratio using a high-temperature, high-pressure methanol-synthesis catalyst promoted with K. The catalyst is a commercially available, Zn/Cr spinel catalyst, Engelhard Zn-0312, which has been impregnated with varying amounts of K. Reaction studies were performed using each of the catalysts made at two different temperatures and two pressures in order to determine the optimum promotor concentration and preferred reactor operating conditions. X-ray photoelectron spectroscopy (XPS) and ion-scattering spectroscopy (ISS) were used to examine the fresh, pretreated and aged catalyst surfaces before and after sputtering in order to determine compositional and chemical-state information regarding the near-surface region of the catalyst. This was done in an attempt to relate the surface chemistry to the reactivity data.

Experimental

Reaction Studies

The Zn/Cr spinel support was purchased from Engelhard Industries (Engelhard Zn-0312). The bulk Zn-to-Cr wt. ratio in this spinel is 3:1, and the O content is 21 wt.%. The catalysts were impregnated with 1, 3 and 5 wt.% K using potassium nitrate and the incipient wetness method. The reactor consisted of a 1/4" copper tube inserted into a 3/8" stainless steel tube. This arrangement eliminates products which form due to feedstream reactions with the stainless steel at the elevated temperatures. One gram of catalyst was mixed with three grams of glass beads for catalyst dispersion and then placed into the reactor tubes. These tubes were placed into an air fluidized sandbath which was used for

heating. The feed and pretreatment gases were passed through a molecular-sieve-activated carbon trap to remove water and metal carbonyl contaminants before entering the reactant tube. The catalysts were calcined in air at 325°C to stabilize the material and then reduced with a 5% hydrogen-in-nitrogen mixture for four hours at 300°C. The reactions were run using a feed gas of a 1:1 H_2 and CO mixture at a space velocity of 12,000. The reactions were run at two different temperatures, 400 and 440°C, and pressures, 1000 and 1500 psig. The product stream was analyzed using a Varian 3700 gas chromatograph. Inorganics were detected by thermal conductivity measurements using a Carbosieve S-2 column purchased from Supelco. The organic products were detected using a 12 ft, 1/8", 80/100 Tenax column obtained from Alltech which was calibrated on an absolute weight basis using quantified mixtures of C_1-C_6 normal hydrocarbons, normal and branched alcohols and normal aldehydes. Argon was used as the carrier gas in both columns.

Characterization Studies

The fresh catalyst material (unreacted) was pressed into an Al cup and inserted into an ultra-high vacuum chamber (base pressure of $<10^{-10}$ Torr) to carry out the surface characterization studies. The XPS and ISS data were collected using a double-pass cylindrical mirror analyzer (CMA) (PHI Model 15-255 GAR). The CMA was operated in the retarding mode with pass energies set at 25 eV for the high-resolution XPS spectra and 50 eV for the XPS survey spectra. A Mg Kα X-ray generator was used as the excitation source. Binding energy (BE) values were determined by assigning the Fermi level to 0.0 eV and then ensuring the Zn 2p peak of ZnO has a BE value of 1021.7 eV (58). The ISS was performed using 1-keV He^+ defocused over a spot size of 0.5 cm^2. A total-ion current of 100 nA was used, and each spectrum was collected in 66 seconds. These operating conditions result in minimal sputter damage. The CMA was operated in

the nonretarding mode during collection of the ISS spectra, and both XPS and ISS data were collected using pulse-counting detection (59).

After the initial surface characterization was accomplished, the fresh catalysts were reduced for 4 hours in $1x10^{-7}$ Torr of flowing research-grade H_2. The temperature was ramped at approximately 2°C per minute to 250°C and held at this temperature for the remaining time. The pretreated catalyst was then reanalyzed using XPS and ISS without exposure to air after the pretreatment. A depth profile was obtained by sputtering the sample with a 1-keV beam of 1:1 He^+ and Ar^+ for varying intervals of time while ISS spectra were collected. Chemical-state analysis was again performed using XPS to examine the chemical states of the species present after sputtering. The aged catalysts were retrieved from the reactor after functioning for about one week under reaction conditions. These samples also were characterized using XPS, ISS and depth profiling.

Results and Discussion

Reaction Studies

A detailed listing of the product distribution using a nonpromoted and 1, 3 and 5 wt.%-K promoted catalysts under 4 sets of reaction conditions is shown in table 2-1. Since the highest isobutanol rates and lowest methanol-to-isobutanol mole ratios are attained using a pressure of 1500 psi and 440°C for each catalyst except the 5 wt.% K-containing sample, these seem to be the most favorable conditions of the four tested. The higher temperature, however, results in a loss of selectivity due to a higher hydrocarbon product rate. The higher pressure slightly increases the selectivity of the nonpromoted and 5 wt.% K-containing catalyst and significantly increases the overall product rates over each of the catalysts. Small amounts of other alcohols also are produced, but isobutanol and methanol are consistently the primary alcohol products. The product stream composition obtained using the 3 wt.%-K catalyst at 400°C and 1000 psi as a function of time is given in table 2-2. Little variation is noticable after 15 hrs on stream,

and no trends in the product rates are evident other than the formation of n-propanol after 13 hrs. Each catalyst was tested at each of the 4 operating parameters listed for a minimum of 24 hours. No significant changes in catalyst activity or product stream compositions were noted at any of the conditions tested.

The total alcohol rate as a function of K loading at 440°C and 1500 psi is shown in figure 2-1a. The use of the 1 wt.% K-containing catalyst results in the highest alcohol rate. The nonpromoted catalyst can produce significant quantities of alcohols, but the product stream is composed primarily of methanol and very little isobutanol as shown in figure 2-1b. The total alcohol rate increases initially upon the addition of K but decreases to 99 g/kg-hr with the addition of 3 wt.% K to the spinel and increases again to 130 g/kg-hr upon addition of 5 wt.% K. The addition of K increases the isobutanol production rate, and a maximum is achieved with the 1 wt.%-K catalyst. [A product stream flowrate of← 103 g/kg-cat/hr of isobutanol is greater than that attained by Beretta et al. (41) using a $Cs/ZnO/Cr_2O_3$ catalyst.] The use of the 1 wt.% K catalyst also results in a methanol-to-isobutanol mole ratio of 1.9, while an ever lower ratio is achieved, 1.5, when using the 3 wt.%-K catalyst. The effect of the addition of K on the selectivity to total alcohols is shown in figure 2-2a. The highest selectivity to total alcohols is attained using the 5 wt.%-K catalyst and decreases as the K loading decreases to 1 wt.%. The use of the nonpromoted catalyst results in the lowest selectivity of 43%. As shown in figure 2-2b, the addition of 1 wt.%-K to the Zn/Cr spinel slightly increases the formation of hydrocarbon byproducts. Increasing the amounts of K further, however, results in a decrease in the amount of hydrocarbons produced which accounts for the increase in alcohol selectivity observed in figure 2-2a. Surface science analysis was performed on the Zn/Cr spinel catalyst containing 3 wt.% K since its use led to the lowest methanol-to-isobutanol mole ratio under the conditions used.

Characterization Studies

Ion scattering spectroscopy is an important surface science technique in catalysis due to its extremely high surface sensitivity. This technique yields compositional information about the outermost atomic layer, which is where the catalytic reactions occur. An ISS spectrum taken from the fresh 3 wt.% K-promoted catalyst is shown in figure 2-3a. A predominant feature due to charging is present at an E/E_o of 0.46. Features due to O and C also are apparent at E/E_os of 0.38 and 0.27, respectively. Upon expanding the intensity of the higher E/E_o region of the spectrum by a factor of 5, Cr and Zn peaks become evident. This spectrum indicates that the as-prepared catalyst surface contains mostly O in the outermost atomic layer. The charging feature which is present in these spectra is most likely caused by the presence of large amounts of O at the surface which results in an insulating surface layer and could lead to the charging features observed. Features due to charging typically occur on the lower portions of ISS spectra and therefore may have effects on C and O peak positions and intensities. The features due to heavier elements lie at higher E/E_o values, and the separation between their peaks diminishes as the atomic weight increases. Due to this, these features are less affected by any charging features in these spectra other than their appearance as small peaks due to the large size of the charging peak. After exposing the catalyst to 1×10^{-7} Torr of H_2 for 4 hrs at 250°C, the ISS spectrum shown in figure 2-3b was taken. This treatment is similar to the pretreatment conditions used on the catalysts before they are exposed to the reaction stream. The charging feature is still apparent, but at a lower E/E_o and is much sharper. Many variables would define the peak shapes and positions caused by sample charging and as of yet no research has been accomplished on the development of models which would lead to an understanding of these features. The primary component of the outermost surface layer of this sample is K, and the Zn and Cr peaks are not evident. This indicates that the H_2 treatment removes surface O exposing underlying K. Also some K may have migrated to the surface and over the surface covering the underlying

Zn and Cr. The ISS spectrum shown in figure 2-3c was taken after the catalyst was sputtered with 1-keV He^+ for 5 minutes. A significant Zn feature is now evident indicating that the sputtering process removes some K from the surface, exposing a small amount of Zn located beneath the K layer. Another ISS spectrum shown in figure 2-3d was taken after sputtering the sample for 15 min with 1-keV 1:1 He^+ and Ar^+. Most of the K layer is sputtered away. The primary feature is due to Zn at the surface, a smaller Cr feature is evident, and a small feature due to O may be apparent. A feature due to subsurface Na contamination is also apparent. A previous study reported that the O/Ag ISS cross section ratio is 0.05 (60). Although Zn is smaller in weight than Ag, this value shows that small O peaks could indicate large amounts of O at the surface. Indeed, there appear to be small O features in the spectra shown in figures 2-3c and 2-3d, demonstrating that the Zn and Cr at the sample surface may be in oxidic form. The collection of an ISS spectrum using He^+ and the operating parameters used would result in the removal of less than one-tenth of a monolayer. This indicates that small O features would not be due to the removal of O by the sputtering process.

Surface analysis was performed on the aged catalysts after they had been in the reactor for about 5 days. The reaction data did not vary over this time period unless the operating parameters were adjusted to test another setting. The catalytic properties of these samples remain stable with time during the intervals used. An ISS spectrum taken from the aged 3-wt.% K Zn/Cr spinel catalyst is shown in figure 2-4a. The outermost surface layer of this sample is changed significantly from those of the as-prepared and pretreated catalysts. Features due to K, Cr and Zn are all present, and a large Na peak is evident also. This indicates that the Na which is present in the near-surface region, but not at the surface, of the pretreated sample migrates toward the surface of the sample as the reaction proceeds or that the K may have agglomerated exposing the underlying Zn, Cr and Na. Sputtering the sample results in an increase in the surface Zn concentration as seen in figure 2-4b, and a small peak at an E/E_0 of approximately 0.64 is caused by the

presence of S contamination at the surface. The ISS spectrum shown in figure 2-4c was taken after sputtering the sample for an additional 15 min with 1-keV 1:1 He+ and Ar^+. Much of the K and Na is removed by the sputter process. A small peak at an E/E_o value of 0.46 is due to O. This feature is shifted to a higher E/E_o by charging and as discussed previously, the higher lying features due to the heavier elements are much less affected by the charging. The primary peak in this spectrum is due to Zn while a small shoulder is observable which indicates that some Cr is present as well. This spectrum is similar to that shown in figure 2-3d.

An XPS survey spectrum taken from the fresh catalyst is shown in figure 2-5. Predominant peaks due to Zn and O are readily apparent, and small Cr and C features also are present. The Cr features are much smaller than the Zn features indicating that the near-surface region of the catalyst is enriched in Zn with only a trace amount of Cr present. The carbon is a contaminant formed by exposure to air. Similar survey spectra were obtained from the reduced and aged catalysts and therefore are not presented. The most significant difference in the survey spectra is that the Cr 2p peaks are larger by a factor of about 2 after reduction of the fresh catalyst, are larger by a factor of about 3 for the aged catalyst and doubled again after sputtering the aged catalyst.

A high-resolution XPS Zn 2p spectrum taken from the fresh catalyst is shown in figure 2-6a. The only chemical state of Zn present in the near-surface region appears to be ZnO (58). In fact, ZnO is the primary or only state of Zn present in the near-surface region of all the catalyst surfaces examined (figure 2-6a-e) in this study. An interaction between Cu and Zn produces a peak with a BE value which is 0.7 eV less than that of ZnO (61). A similar shift would be expected if a Cr-Zn alloy were present, but no such feature is noticeable, but would be difficult to detect since the ZnO peak is large. This fact would hinder observing a feature 1022.1 eV due to $ZnCr_2O_4$ (62) also. The FWHM of all the Zn 2p features in figure 2-6 are similar as are their peak shapes. This supports the assertion that only one chemical state of Zn such as ZnO is present. These data also

indicate that the Zn/Cr spinel does not play an active role in the catalytic process in HAS since no Zn-Cr spinel features are evident. The reaction process seems not to be based on the presence of the spinel, although the spinel may contribute to the activity solely as a high surface area support material.

A high-resolution XPS O 1s spectrum taken from the fresh catalyst is shown in figure 2-7a. The broad peak width indicates that a mixture of chemical states is present. Zinc oxide and hydroxyl groups are the primary contributors to this signal, and a small amount of adsorbed water as well as some chemisorbed O also are present. The assignment of this low BE feature is based on a previous study of the thermal decomposition of silver (63). After reducing the sample, the O 1s spectrum shown in figure 2-7b was taken. The contribution from OH is greatly diminished, but a small, well-defined shoulder due to adsorbed H_2O is apparent. The removal of the OH groups contributes to the exposure of more of the ZnO and possibly more catalytic sites. Sputtering the sample does not alter the O 1s peak significantly, as shown in figure 2-6c, but the adsorbed H_2O peak size is reduced. The O 1s spectrum taken from the aged catalyst is shown in figure 2-6d. Significant changes have occurred due to the reacion process. The primary feature still is assigned to ZnO, but the size of the chemisorbed O feature is now increased and the hydroxyl group concentration is increased significantly. As shown in figure 2-7e, sputtering does not alter the O 1s feature very much indicating that the composition of the near-surface region is fairly uniform with respect to the O species present. The chemisorbed O feature is slightly larger which is probably due to the sputtering process which could cause the oxides to decompose leading to a greater amount of chemisorbed O.

The XPS C 1s spectrum taken from the fresh catalyst is shown in figure 2-8a. The primary feature has a BE of 284.4 eV which is assigned as due to hydrocarbons. These catalysts had been exposed to air which typically results in accumulation of hydrocarbon contamination at the surface. A small K $2p_{3/2}$ peak also is apparent at a BE of 293.0 eV.

A previous XPS study of $K_2Cr_2O_7$ has shown that its K $2p_{3/2}$ peak has a BE of 292.8 eV (64), and the BE value of the K $2p_{3/2}$ peak obtained from K_2CrO_4 is 292.6 eV (65). The Cr 2p XPS spectrum taken from the fresh catalyst is shown in figure 2-9a. The primary peak has a BE of 579.6 eV which also can be assigned as $K_2Cr_2O_7$ (66,67). These data indicate that a K-Cr complex exists in the near surface region of the fresh catalyst.

An XPS C 1s and K 2p spectrum obtained from the reduced catalyst is shown in figure 2-8b. The C 1s peak is greatly reduced in size, and the K 2p peaks are increased in size. The reductive pretreatment nearly eliminates the carbon contamination in the near-surface region and causes K to migrate toward the surface. Even though XPS is much less surface sensitive than ISS, these data are consistent with the ISS data discussed above which indicate that the outermost surface layer of this sample is composed primarily of K. The BE values of both the K 2p features and Cr 2p features (figure 2-9b) can be assigned as potassium dichromate or potassium chromate as discussed above. The Cr 2p peaks are more than doubled in size due to this treatment also. This increase in the Cr 2p peak sizes was noticed in the XPS survey spectrum taken from this sample as well. The reactivity data shown in Table 2-1 demonstrates the necessity of K in order to attain isobutanol production. The XPS and ISS data both indicate that the K is present at the surface, possibly associated with the Cr after the reductive pretreatment is performed. Furthermore, the XPS data show that C and some O contamination is removed by this treatment as well which may result in the exposure of a greater number of active sites. After sputtering the catalyst with 1-keV He^+ for 5 min and 1-keV 1:1 He^+ and Ar^+ for 20 min, the spectra shown in figures 2-8c and 2-9c, respectively, were taken. The K 2p peak is shifted to a lower BE, probably due to partial decomposition of the $K_2Cr_2O_7$ or $KCrO_4$. The Cr 2p spectrum obtained after sputtering contains features due to the presence of $Cr(OH)_x$, Cr_2O_3 (68) and potassium chromate. The former Cr species form upon decomposition of the potassium chromate or by exposure of Cr in the underlying substrate as the K-containing layer is sputtered away.

A C 1s and K 2p spectrum taken from the aged catalyst is shown in figure 2-8d. Features due to K and C are no longer apparent before or after sputtering (figure 2-8e). The XPS Cr 2p spectrum obtained from the aged catalyst is shown in figure 2-9d. Significant changes in the near-surface region have occurred during the reaction process. The predominant peak due to potassium chromate present in the spectra taken from the fresh catalyst is decreased significantly in size. The primary peak is now assigned to Cr_2O_3 and $Cr(OH)_x$, and a small Cr^o signal also is apparent. Sputtering the aged sample reduces some of the Cr_2O_3 to Cr^o as shown by comparing figure 2-9d and e. Chromium hydroxide species also are exposed which initially are present beneath the outermost surface layers. Although no significant changes in catalytic activity were noticed between the beginning and end of the experimental runs, the XPS data indicate that K is no longer at the sample surface which would seem necessary to maintain the activity. The ISS data presented earlier, however, depict an outermost surface layer which contains a significant quantity of K. The two techniques, XPS and ISS, probe different depths which accounts for this apparent discrepancy between the results. The amount of K in the near-surface region has decreased below the sensitivity of XPS; however, the amount at the outermost surface layer is detectable by ISS.

Summary

A commercially available Zn/Cr spinel methanol-synthesis catalyst (Englehard Zn-0312) has been promoted with various amounts of K and tested for isobutanol synthesis. The best operating parameters for the 1 and 3 wt.%-K catalyst are the higher temperature and pressure settings of 440°C and 1500 psi. The total alcohol rate initially increases upon adding K, as does the isobutanol rate which achieves a maximum with the addition of 1 wt.%-K. The methanol and hydrocarbon rates also decrease with increasing K above 1 wt.% although the 5 wt.%-K catalyst does produce a slightly higher amount of methanol than the 3 wt.%-K catalyst. The use of the 3 wt.%-K catalyst at 440°C and

1500 psi results in the lowest methanol-to-isobutanol mole ratio of 1.5. An isobutanol product rate as high as 103 g/kg-cat/hr is achieved using the Zn/Cr spinel promoted with 1 wt.% K. The near-surface region of the fresh catalyst is found to be composed primarily of ZnO and a small amount of hydrocarbon contamination. Reducing the catalyst at 250°C for 4.5 hrs in 1 x 10^{-7} Torr of H_2 eliminates the C from the near-surface region and induces the K to cover the ZnO at the topmost surface region. The K is associated with Cr as potassium chromate or dichromate. The active catalyst sites may be the K which lies over the ZnO. No Zn/Cr spinel structures were observed which indicates it may only act as a support material not as the catalyst. The aged catalyst, which was removed from the reactor after a 5-day test period, contains very little K in the near-surface region, and the Cr is present as Cr_2O_3, $Cr(OH)_x$ and Cr^0. The outermost surface layer still contains K according to the ISS data, however. The primary component of the aged catalyst is ZnO also.

Table 2-1. Zn/Cr Engelhard Spinel containing

	0% K				1% K				3% K				5% K			
P (psi) T (°C)	1000 400	1500 400	1500 440	1000 440	1000 400	1500 400	1500 440	1000 440	1000 400	1500 400	1500 440	1000 440	1000 400	1500 400	1500 440	1000 440
Selectivity to Total Alcohols (%)	65	77	43	27	61	75	53	53	80	88	70	70	96	97	84	83
Total Alcohol Rate (g/kg-hr)	111	236	133	59	133	251	167	129	75	159	99	67	82	159	130	70
Methanol Rate (g/kg-hr)	105	223	102	41	78	170	49	70	38	92	26	8	59	123	47	16
Ethanol Rate (g/kg-hr)	0	0	0	0	0	0	0	0	0	0	0	0	0	0	0	0
Isopropanol Rate (g/kg-hr)	0	0	0	3	0	0	6	5	0	1	6	2	0	1	9	5
n-Propanol Rate (g/kg-hr)	0	0	18	10	8	0	9	6	4	10	0	0	0	0	23	10
Isobutanol Rate (g/kg-hr)	6	13	13	5	47	81	103	47	34	57	67	57	23	34	51	38
MetOH/i-ButOH mole ratio	73	68	31	36	6.6	8.4	1.9	6.0	4.5	6.4	1.5	0.54	10	14	3.7	1.7
Hydrocarbon Rate (g/kg-hr)	30	35	94	86	48	46	101	65	11	12	29	21	2	3	15	10
Conversion (%)	8	14	14	9	12	19	19	13	10	12	13	11	13	14	15	13

Table 2-2. The product stream analysis using the Zn/Cr Engelhard Commercial Spinel Support plus 3 wt% K at 400 °C and 1000 psi as a Function of Time.

	Time on stream (hours)						
	3	5	7	9	11	13	15
Sel. Total Alcohols (%)	78	80	79	77	76	79	80
Total Alcohol Rate (g/kg-hr)	70	77	76	67	65	76	75
Methanol Rate (g/kg-hr)	33	37	38	40	40	39	38
Ethanol Rate (g/kg-hr)	0	0	0	0	0	0	0
Isopropanol Rate (g/kg-hr)	0	0	0	0	0	0	0
n-Propanol Rate (g/kg-hr)	0	0	0	0	0	4	4
Isobutanol Rate (g/kg-hr)	36	40	38	27	25	33	34
MeOH/i-BuOH Mole Ratio	3.7	3.8	4.0	5.8	6.3	4.7	4.5
Hydrocarbon Rate (g/kg-hr)	12	12	12	11	11	12	11
Conversion (%)	10	10	10	10	10	10	10

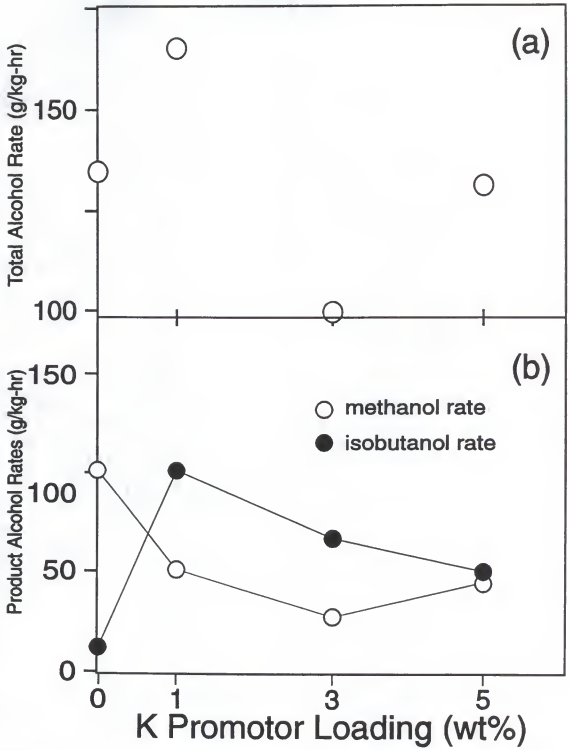

Figure 2-1. The effect of K loading when the reactor is operated at 440°C and 1500 psi on a) the total alcohol rate; b) the methanol and isobutanol rates of the product stream.

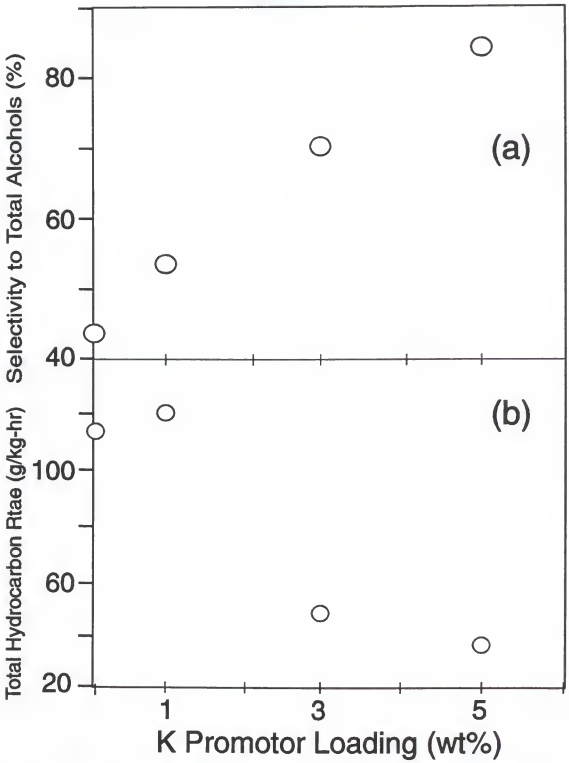

Figure 2-2. The effect of K loading when the reactor is operated at 440°C and 1500 psi on a) the selectivity to total alcohols; b) the total hydrocarbon rate.

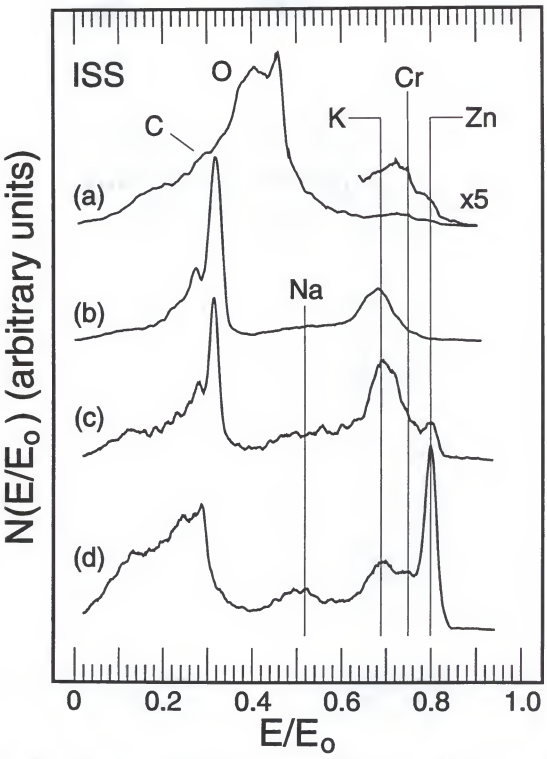

Figure 2-3. ISS spectra taken from the 3 wt.% K/Zn/Cr spinel catalyst after a) insertion into the UHV system; b) pretreating in 1 x 10^{-7} Torr of H_2 for 4 hrs at 250°C; c) sputtering for 5 min with 1-keV He^+; d) sputtering for another 15 min with 1-keV 1:1 He^+ and Ar^+.

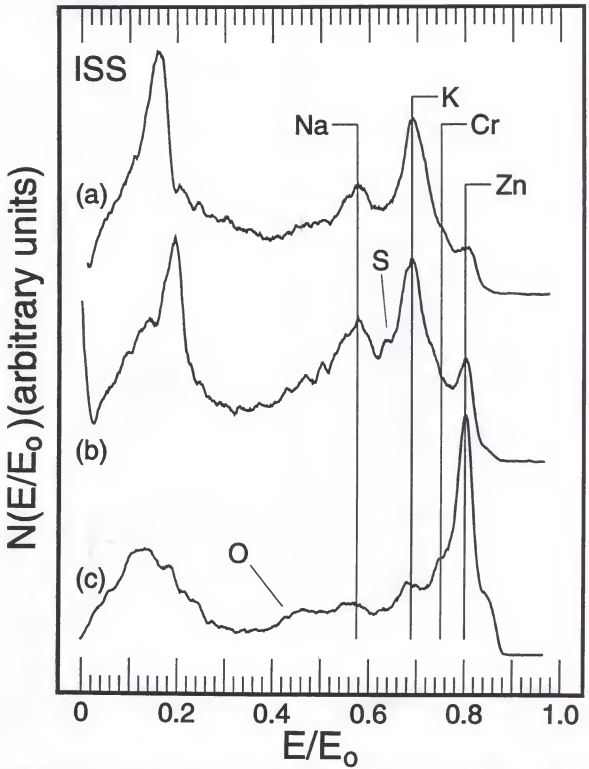

Figure 2-4. ISS spectra taken from the aged 3 wt.% K/Zn/Cr spinel catalyst after a) insertion into the UHV system; b) sputtering for 5 min with 1-keV He^+; c) sputtering for another 15 min with 1-keV 1:1 $He^+$and Ar^+.

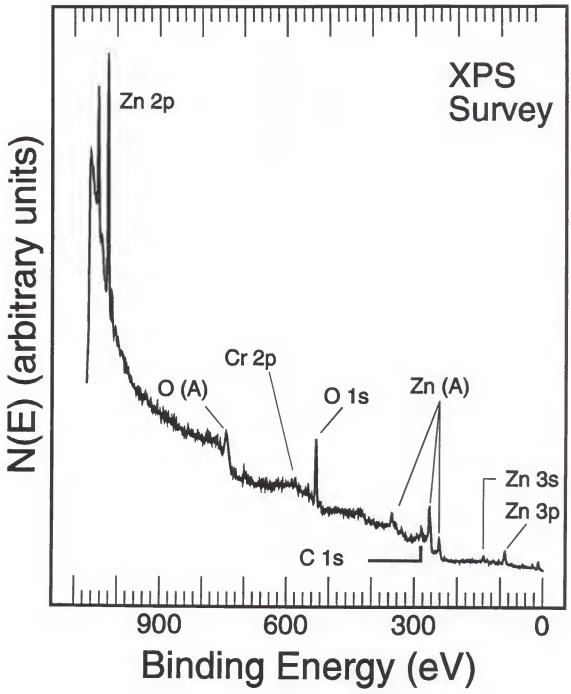

Figure 2-5. XPS survey spectrum taken from the nonreacted, nonpretreated, 3 wt.% K/Zn/Cr spinel catalyst.

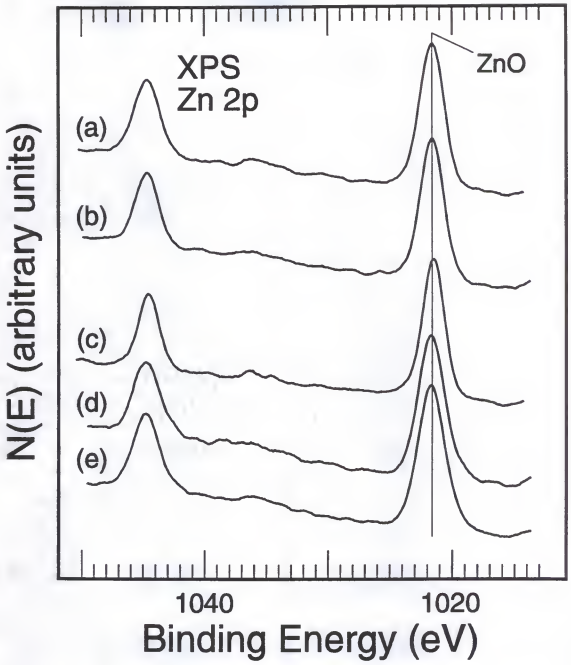

Figure 2-6. XPS Zn 2p spectra taken from the 3 wt.% K/Zn/Cr spinel catalyst after a) insertion into the UHV system; b) pretreating in 1 x 10^{-7} Torr of H_2 for 4 hrs at 250^{0}C; c) sputtering for 5 min with 1-keV He^+ and 15 min with 1-keV 1:1 He^+ and Ar^+: d) the aged 3 wt.% K/Zn/Cr spinel catalyst; e) the aged catalyst after sputtering for 5 min with 1-keV He and 15 min with 1-keV He^+ and Ar^+.

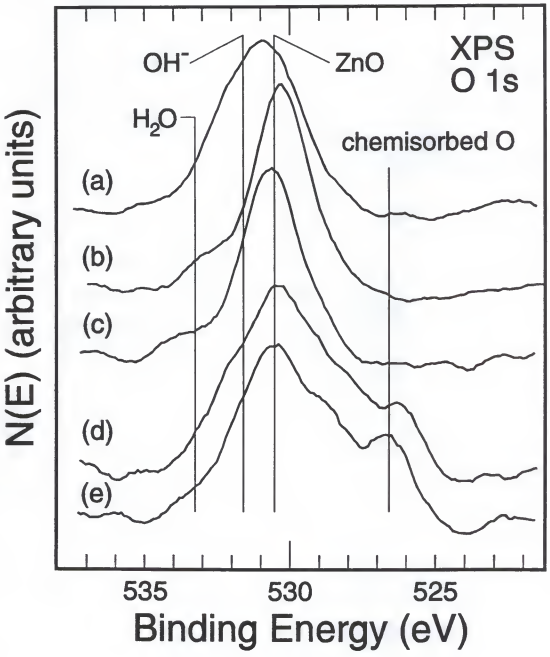

Figure 2-7. XPS O 1s spectra taken from the 3 wt.% K/Zn/Cr spinel catalyst after a) insertion into the UHV system; b) pretreating in 1 x 10^{-7} Torr of H_2 for 4 hrs at 250°C; c) sputtering for 5 min with 1-keV He^+ and 15 min with 1-keV 1:1 He^+ and Ar^+; d) the aged 3 wt.% K/Zn/Cr spinel catalyst; e) the aged catalyst after sputtering for 5 min with 1-keV He^+ and 15 min with 1-keV He^+ and Ar^+.

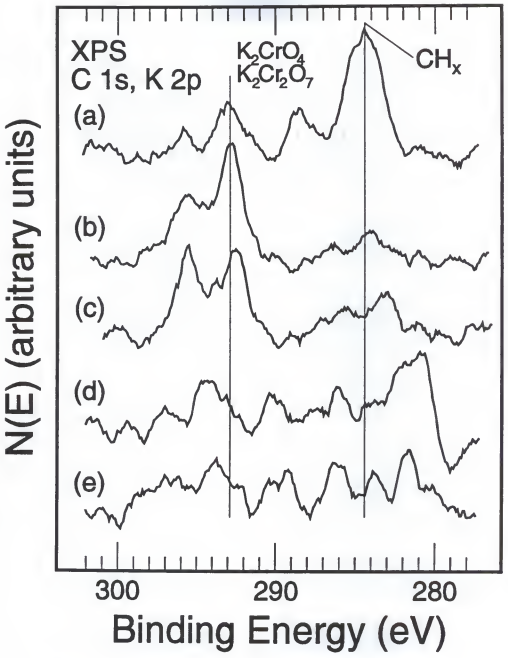

Figure 2-8. XPS C 1s and K 2p spectra taken from the 3 wt.% K/Zn/Cr catalyst after a) insertion into the UHV system; b) pretreating in 1 x 10^{-7}Torr of H_2 for 4 hrs at 250°C; c) sputtering for 5 min with 1-keV He^+ and 15 min with 1-keV 1:1 He^+ and Ar^+: d) the aged 3 wt.% K/Zn/Cr spinel catalyst; e) the aged catalyst after sputtering for 5 min with 1-keV He^+ and 15 min with 1-keV He^+ and Ar^+.

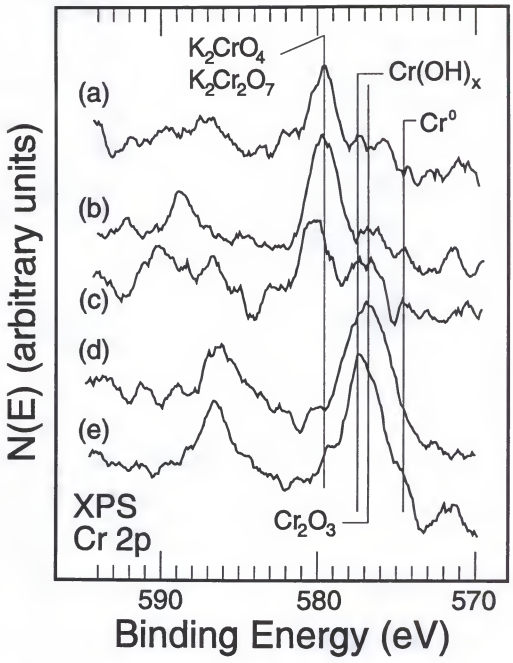

Figure 2-9. XPS Cr 2p spectra taken from the 3 wt.% K/Zn/Cr spinel catalyst after a) insertion into the UHV system; b) pretreating in 1 x 10^{-7} Torr of H_2 for 4 hrs at 250°C; c) sputtering for 5 min with 1-keV He^+ and 15 min with 1-keV 1:1 He^+ and Ar^+; d) the aged 3 wt.% K/Zn/Cr spinel catalyst; e) the aged catalyst after sputtering for 5 min with 1-keV He^+ and 15 min with 1-keV He^+ and Ar^+.

CHAPTER 3
STUDY OF A Cs-PROMOTED COMMERCIAL Zn/Cr SPINEL FOR HAS

In this chapter the optimization of isobutanol production and the methanol-to-isobutanol mole ratio using a Cs-promoted, Engelhard Zn/Cr spinel, methanol synthesis catalyst has been examined. Two different operating pressures (1000 and 1500 psi) and two different operating temperatures (400 and 440°C) were used in order to examine the effects of temperature and pressure on catalyst performance. The effects of Cs loading also were studied. The fresh, pretreated and aged catalyst surfaces were examined with ISS and XPS before and after depth profiling in order to determine chemical-state and compositional information of the near-surface region of the samples.

Experimental

The Zn/Cr spinel catalyst was purchased from Engelhard Industries (Zn 0312). The catalyst samples were impregnated with 1, 3 and 5 wt% Cs using the incipient wetness technique with cesium nitrate as the precursor. Each of these catalysts as well as the nonpromoted Zn/Cr spinel then were pretreated as described in the previous chapter. The details of the reactor and characterization experiments have been described previously as well.

Results and Discussion

Reaction Studies

The compositions of the product streams obtained using a nonpromoted, 1, 3 and 5 wt%-Cs-containing catalyst at 4 different sets of operating parameters and a 1:1 feed mixture of CO and H_2 are listed in table 3-1. An increase in the reactor bed temperature results in an increase in the selectivity to total alcohols for all catalysts but the 3 wt% Cs

sample. This selectivity increase can be attributed to a sharp increase in the total alcohol production rate as the temperature is increased from 400°C to 440°C. The isobutanol production rate is greatest when both the temperature and pressure are at the higher values tested. Furthermore, increasing the temperature at a pressure of 1500 psi decreases the methanol production rate resulting in a lower methanol-to-isobutanol mole ratio. The highest isobutanol production rates consistently occur when the reactor is operated at 440°C and 1500 psi. Therefore, these conditions are the best settings of those tested for maximizing the isobutanol production rate. Similar results were reported using the K-promoted Zn/Cr catalysts under identical reaction conditions. It is unfortunate, however, that the hydrocarbon-byproduct rate is greatest at these operating parameters as well.

The effect of Cs loading on the product stream composition was tested also. The total alcohol production rate as a function of promotor loading at 440°C and 1500 psi is shown in figure 3-1a. A maximum total alcohol production rate of 214 g/kg-hr is achieved using the 3 wt%-Cs-containing catalyst. Further addition of Cs to 5 wt%, however, results in a sharp decrease in the total alcohol production rate. The separate isobutanol and methanol production rates are shown in figure 3-1b. The addition of 1 wt% Cs to the spinel greatly increases the isobutanol production rate and decreases the methanol production rate. Increasing the Cs-promotor loading to 3 wt% results in a slight increase in the isobutanol production rate to 116 g/kg-hr, but an increase in the methanol production rate occurs as well. This increases the methanol-to-isobutanol mole ratio from 1.1 to 1.7. Using the 5 wt%-Cs-containing catalyst significantly decreases the isobutanol production rate which coincides with the sharp decrease in the total alcohol production rate mentioned above. The effect of Cs addition on the selectivity to total alcohols is shown in figure 3-2a. Promoting the spinel catalyst with Cs increases the selectivity toward total alcohol production, and a maximum occurs using the 3 wt%-Cs-containing catalyst. As shown in figure 3-2b, increasing the amount of Cs results in a monotonic

decrease of hydrocarbon byproduct rate. Hence, the selectivity decrease upon the addition of 5 wt% Cs is attributed solely to the decrease in the isobutanol production rate. Overall, the addition of Cs results in improved catalyst performance upon comparison with the K-promoted catalysts. A greater total alcohol production rate, isobutanol production rate and higher selectivities to alcohol are achieved using Cs as the promotor rather than K. Furthermore, lower methanol-to-isobutanol mole ratios can be obtained using the appropriate reaction conditions. Surface-science analysis was performed on the Zn/Cr spinel catalyst containing 3 wt% Cs because the highest isobutanol production rate, highest total alcohol production rate and greatest selectivity to alcohols is achieved using this catalyst. The examination of this catalyst also can be compared to the 3 wt.% K catalyst examined in the previous chapter.

Characterization Studies

The high surface sensitivity of ISS makes it a very useful surface analysis technique particularly when used in conjunction with less surface sensitive techniques such as XPS. In catalysis information concerning the outermost surface is very important since the reactions occur at the outermost catalyst surface which makes ISS particularly useful. An ISS spectrum taken from the fresh 3 wt%-Cs-containing catalyst is shown in figure 3-3a. A large feature is present at an E/E_0 value of approximately 0.34 due to C, and a shoulder is present at an E/E_0 of 0.42 due to O. These values are higher than predicted by the elastic binary scattering equation due to charging as evidenced by the low-energy feature at an E/E_0 of 0.18. Upon expanding the region between E/E_0 values of 0.74 and 0.96 by a factor of 5, features due to the presence of Cs and Zn are observable. The spectrum shown in figure 3-3b was taken from the 3 wt% Cs-promoted catalyst after exposure to $1x10^{-7}$ Torr of H_2 for 4 hrs at 250°C which is similar to the pretreatment used on the catalysts before reaction studies. The charging feature remains at an E/E_0 of about 0.2 but is diminished in size. A large Cs peak is evident and Zn and

Cr features are also present, but they are much smaller than the Cs peak. The data indicate that Na and Cl contaminants are present on this surface also. The O feature is small, but due to the low cross section of O in ISS, this small signal still indicates that a substantial surface concentration of oxygen is present. After sputtering the pretreated catalyst for 5 min with 1-keV He^+, the spectrum shown in figure 3-3c was taken. The Zn feature is increased in size relative to the Cs peak indicating that Cs removal exposes underlying Zn. Furthermore, the Cr feature is larger than in figure 3-3b. The Cl peak is no longer evident and the Na feature is decreased somewhat. After sputtering the sample for an additional 15 min with 1-keV 1:1 He^+ and Ar^+, the spectrum shown in figure 3-3d was obtained. The Cs peak is now relatively small, and the Zn and Cr features are increased in size. Furthermore, the background signal is diminished indicating that the surface is more conductive or less oxidic as evidenced by the lack of an O feature at E/E_o of 0.37. This series of ISS spectra closely resemble those taken from the K-promoted catalyst presented in the previous chapter in which the outermost surface layer of the fresh catalysts are composed primarily of oxygen and a reductive pretreatment results in coverage of the surface with K.

Surface analysis also was performed on the catalysts after exposure to the reactant stream for 5 days. An ISS spectrum taken from an aged, 3 wt% Cs catalyst is shown in figure 3-4a. Again, a large charging feature is apparent at the lower E/E_o values which indicates the outermost surface layer contains substantial amounts of oxygen and carbon. The Cs and Zn features are present, and the Cs-to-Zn ratio does not differ significantly from that obtained from the pretreated catalyst (figure 3-3b). A small amount of Cl also is apparent at the surface of the aged catalyst. After sputtering the sample for 5 min, the ISS spectrum shown in figure 3-4b was taken. The Zn-to-Cs peak-height ratio is increased significantly, and a small Na peak due to sample contamination is present. Although a Cr feature is apparent, it is quite small in comparison to the Zn peak. Further sputtering of the sample results in a significant decrease in the Cs peak intensity and an

increase in both the Zn and Cr features as shown in figure 3-4c indicating that Cs covers the underlying Zn and Cr. The broad feature extending from an E/E_0 of 0.06 to 0.5 is due to the presence of C and O. These features decrease in size compared to the Zn feature with sputtering. This indicates that the surface layer of the aged catalyst contains large amounts of C and O compared to the pretreated catalyst (figure 3-3b). The changes in shape indicate that the C sputters away more rapidly leaving a better-defined O peak. Another small peak is apparent in these ISS spectra at an E/E_0 below 0.06. This peak is composed of secondary ions and typically is mostly H^+.

An XPS survey spectrum obtained from the fresh, 3 wt.% Cs catalyst is shown in figure 3-5. Features due to Zn, Cs and O are readily apparent as are small Cr 2p peaks. These XPS data and the previously mentioned ISS data indicate that the near-surface region of this sample is enriched in Zn. This result also is consistent with data obtained from the 3 wt%-K-promoted Zn/Cr spinel catalyst. Similar survey spectra were obtained from the pretreated and aged catalysts so they are not presented. The most significant difference in the spectra is the size of the Cr 2p peaks. The Cr 2p peaks are larger after the fresh catalyst sample is reduced and after the aged catalyst is sputtered. These results are consistent with trends shown by the ISS data, but care must be taken in comparing ISS and XPS data because ISS is outermost atomic layer sensitive and XPS probes more than 30 atomic layers beneath the surface with less than 10% of the signal originating from the outermost atomic layer. Subsurface compositional changes detected by XPS may be quite different than outermost atomic layer compositional changes detected using ISS.

A high-resolution, Zn 2p XPS spectrum taken from the fresh catalyst is shown in figure 3-6a. Based on the peak shape and width, ZnO apparently is the only chemical state of Zn present in the near-surface region of the sample. This ZnO feature also is the only peak present in the spectra taken from the pretreated and sputtered samples as shown in figure 3-6b and c. The Zn 2p XPS spectrum taken from the aged catalyst, shown in

figure 3-6d, contains two distinct features. The lower binding-energy (BE) peak is assigned as ZnO. The higher BE peak is due to sample charging since this feature lies beyond the BE range observed in XPS spectra taken from Zn compounds. Sputtering the aged catalyst reduces the intensity of the charging feature as shown in figure 3-6e. This fact indicates that the charged region is at the surface. Peaks other than that due to ZnO would be difficult to detect due to the large intensity of the ZnO peak. Therefore, small amounts of other Zn compounds may be present, but are not distinguishable.

An XPS O 1s spectrum obtained from the fresh catalyst is shown in figure 3-7a. Features due to the presence of several chemical states of oxygen are evident. The predominant peak is assigned as O in ZnO, and the small peak at approximately 527.3 eV is due to chemisorbed oxygen. A small shoulder is evident at 532.8 eV due to the presence of adsorbed water, and the broadening on the high BE side of the O 1s peak indicates that hydroxyl groups are present. Reducing the catalyst at 250°C for 4 hrs in $1x10^{-7}$ Torr of H_2 removes both the adsorbed water and chemisorbed oxygen as shown in figure 3-7b. A contribution by OH^- results in the broadening toward the high BE side of the peak present. After sputtering the pretreated catalyst for 5 min with 1-keV He^+ and for 15 min with 1-keV 1:1 He^+ and Ar^+, the spectrum shown in figure 3-7c was taken. The primary O state is due to ZnO, but hydroxyl groups which initially are beneath the probing depth of XPS are now exposed. An XPS O 1s spectrum taken from the aged catalyst is shown in figure 3-7d. A ZnO feature is evident as is another feature 1.4 eV higher in BE. The charging features present in the Zn 2p spectra taken from the aged catalyst are also higher in BE by 1.4 eV. Therefore the predominant O 1s peak is due to sample charging. Unfortunately, this makes the detection of other oxygen features difficult in both spectra shown in figure 3-7d and e, the spectrum obtained from the aged catalyst after sputtering. The features due to the presence of ZnO in the charged and subsurface regions are evident in the spectra taken from both samples. Sputtering results

in a decrease in the charged O 1s feature similar to the decrease in the charged Zn 3d feature giving further evidence to its presence at the surface.

An XPS C 1s spectrum was obtained from the fresh catalyst and is shown in figure 3-8a. A small feature, barely above the noise level, is apparent at 284.8 eV. This most likely is attributable to the presence of hydrocarbons on the catalyst surface which is typical of air-exposed samples. The C 1s XPS spectrum taken after pretreating the sample in 1 x 10^{-7} Torr of H_2 for 4 hrs at 250°C is shown in figure 3-8b. No C peaks are observable after sputtering the sample so this spectrum is not shown. The spectrum taken from the aged catalyst contains a large C 1s peak as shown in figure 3-8c. This spectrum and the one taken from the aged catalyst after sputtering, shown in figure 3-8d, may be affected by the charging effect noted above thereby making chemical-state assignments difficult. Charging would account for the breadth of the two peaks and the decrease in intensity of the higher BE portion of the peak taken after sputtering. A predominant contribution to these features is due to hydrocarbons, and alcohols most likely contribute also. A smaller peak is present at a BE of 290.0 eV which is due to carbonates. This is shifted to a higher BE by 1.4 eV due to charging. These XPS data are consistent with the ISS data shown in figure 3-4 in which a carbonaceous layer containing O is removed during ISS depth profiling.

The XPS Cs 3d spectrum taken from the fresh catalyst is shown in figure 3-9a. The predominant peak lies at a BE value of approximately 724.9 eV indicating that the Cs is present as Cs_2O (69). A shoulder is also evident at 724.3 eV which is assigned as due to $Cs_2Cr_2O_7$ (65). The Cr 2p XPS spectrum taken from the fresh catalyst, shown in figure 3-10a, also contains a feature due to the presence of $Cs_2Cr_2O_7$ at 579.3 eV (70). Features due to the presence of other Cr states such as Cr_2O_3, $Cr(OH)_x$ and CrO_2 are present as well. The XPS Cs 3d and Cr 2p spectra obtained after reducing the sample are shown in figures 3-9b and 3-10b respectively. The predominant Cs 3d feature is due to cesium dichromate. It is larger than the peak shown in figure 3-9a as is the primary Cr 2p

peak which is also due to the presence of cesium dichromate. Similar to observations made after pretreating K-containing Engelhard Zn/Cr catalysts, the reductive treatment removes surface O and causes a reaction between Cr and Cs to form $Cs_2Cr_2O_7$. Although XPS probes more deeply than ISS, these results are consistent with the ISS results discussed above which indicate that the outermost layer is composed primarily of Cs after the reductive pretreatment. As shown in figures 3-9c and 3-10c, sputtering the sample results in a decrease of the Cs concentration and an alteration in the Cr chemical states to a mixture of oxides. The Cs 3d spectra taken from the aged catalyst before and after sputtering, shown in figure 3-9d and e respectively, are affected by sample charging. Features due to Cs_2O and $Cs_2Cr_2O_7$ are both evident, and the feature due to charging is sputtered away more quickly than those associated with the Zn 2p and O 1s spectra. This may indicate that most of the Cs is located nearer to the surface and not evenly dispersed through the bulk of the sample which also is consistent with the ISS data. The Cr 2p XPS spectrum taken from the aged catalyst, shown in figure 3-10d, contains a mixture of features, most of which are barely discernible above the background although CrO_2 is apparently the predominant feature. Sputtering the aged catalyst results in the exposure of more distinct Cr 2p features as shown in figure 3-10e. Signal contributions due to the presence of $Cr(OH)_x$, CrO_2, CrO_3, Cr_2O_3 and $Cs_2Cr_2O_7$ are all evident.

Summary

A commercially available Zn/Cr spinel, methanol-synthesis catalyst (Engelhard Zn-0312) was promoted with various amounts of Cs and tested for isobutanol and methanol synthesis. The highest isobutanol rates were achieved using the higher temperature and higher pressure settings of 440°C and 1500 psi. However, these reaction conditions also result in the higher hydrocarbon byproduct rates. The total alcohol rate, selectivity to total alcohols and product isobutanol rate increase upon adding Cs and attain a maximum with the addition of 3 wt% Cs. The hydrocarbon byproduct rate

decreases with increasing Cs concentration. The results indicate that a better catalyst for the production of an equimolar mixture of isobutanol and methanol can be achieved by promoting the Zn/Cr spinel with Cs rather than K. Lower methanol-to-isobutanol mole ratios can be obtained as well as higher isobutanol product rates. The near-surface region of the fresh catalyst consists primarily of ZnO and some Cs_2O and $Cs_2Cr_2O_7$. The SEM micrographs of the fresh catalyst show that a fibrous network of particles exists over the Zn/Cr spinel, plated structure. A reductive pretreatment removes O exposing Cs, which almost completely covers the ZnO. The Cs is predominantly in the form of Cs_2O in the fresh catalyst, but after the reductive pretreatment $Cs_2Cr_2O_7$ is the primary chemical state of Cs in the near-surface region. Less Cs and Cr is present in the near-surface region of the aged catalyst which was removed from the reactor after a 5-day test period. The outermost atomic layer of the aged catalyst consists primarily of Cs and a small amount of Cl. The near-surface region of the aged catalysts contains primarily ZnO. The Cr close to the surface is present as CrO_2 and Cr^o while subsurface Cr is present primarily as Cr_2O_3, $Cr(OH)_x$ and CrO_3. The morphology of the catalyst changes with age. The fibrous particles are not evident on the aged catalyst, but small bead-like particles cover most of the underlying Zn/Cr spinel structure.

Table 3-1. Zn/Cr Engelhard Spinel containing

	0 wt% Cs				1 wt% Cs				3 wt% Cs				5 wt% Cs			
P (psi) T (°C)	1000 400	1500 400	1500 440	1000 440	1000 400	1500 400	1500 440	1000 440	1000 400	1500 400	1500 440	1000 440	1000 400	1500 400	1500 440	1000 440
Selectivity to Total Alcohols (%)	65	77	43	27	62	76	57	75	87	91	81	83	97	98	76	62
Total Alcohol Rate (g/kg-hr)	111	236	133	59	100	211	154	69	123	231	214	124	59	164	71	30
Methanol Rate (g/kg-hr)	105	223	102	41	48	119	32	11	56	138	48	18	48	139	27	8
Ethanol Rate (g/kg-hr)	0	0	0	0	0	0	0	0	0	0	10	2	0	0	0	0
Isopropanol Rate (g/kg-hr)	0	0	0	3	0	0	3	2	4	5	10	16	0	0	0	0
n-Propanol Rate (g/kg-hr)	0	0	18	10	0	0	5	2	13	21	20	16	0	0	8	5
Isobutanol Rate (g/kg-hr)	6	13	13	5	52	92	115	57	49	67	116	67	11	25	36	17
MetOH/i-ButOH mole ratio	73	68	31	36	3.8	5.2	1.1	0.8	4.6	8.2	1.7	1.1	17	23	3	1.9
Hydrocarbon Rate (g/kg-hr)	30	35	94	86	36	38	81	62	11	13	35	19	1	2	35	12
Conversion (%)	8	14	14	9	11	16	16	14	15	20	18	15	12	13	18	10

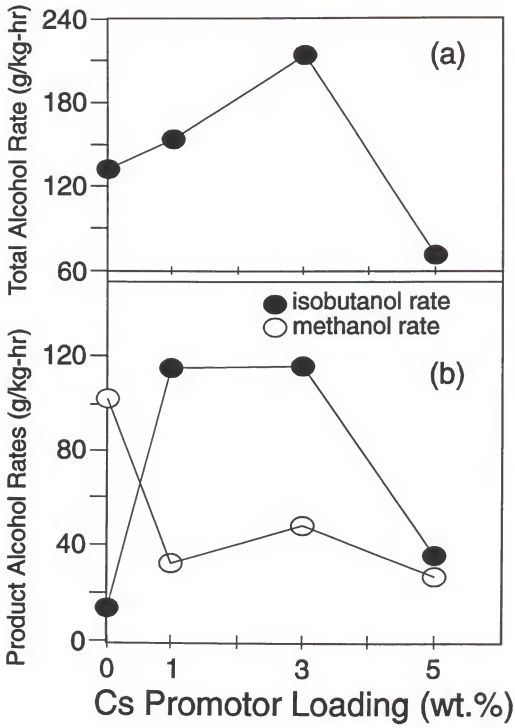

Figure 3-1. The effect of Cs loading when the reactor is operated at 440^{o}C and 1500 psi on a) the total alcohol rate; b) the methanol and isobutanol rates of the product stream.

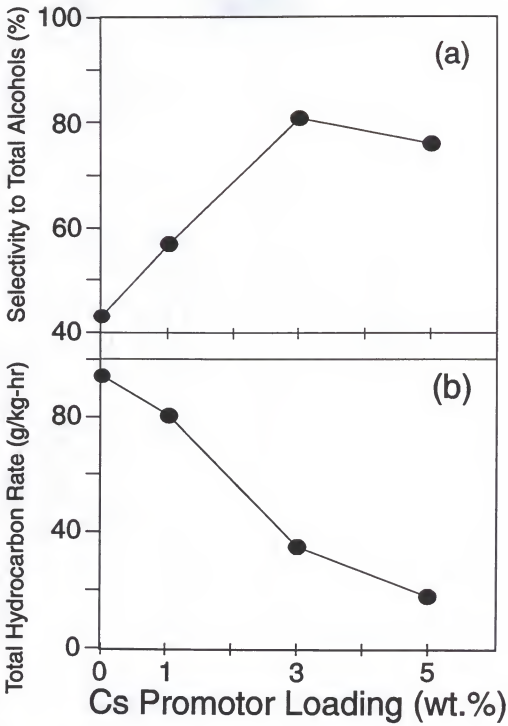

Figure 3-2. The effect of Cs loading when the reactor is operated at 440°C and 1500 psi on a) the selectivity to total alcohols; b) the total hydrocarbon rate.

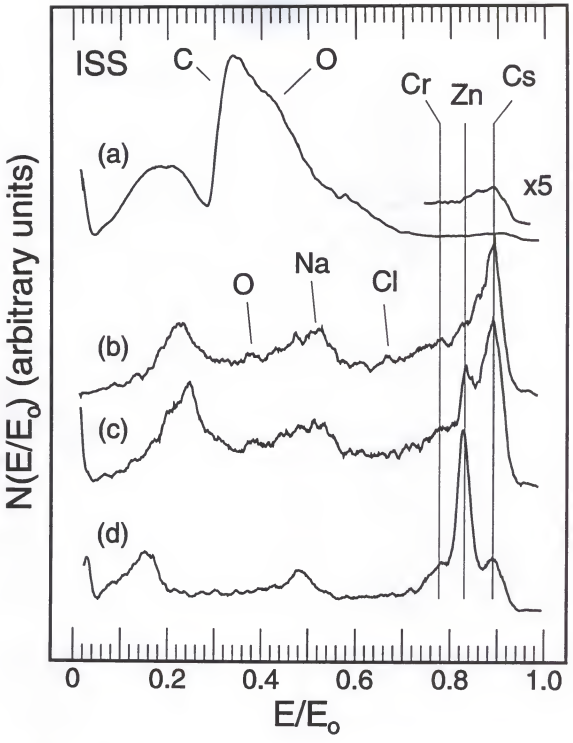

Figure 3-3. ISS spectra taken from the 3 wt.% Cs/Zn/Cr spinel catalyst after a) insertion into the UHV system; b) pretreating in 1 x 10^{-7} Torr of H_2 for 4 hrs at 250°C; c) sputtering for 5 min with 1-keV He^+; d) sputtering for another 15 min with 1-keV 1:1 He^+ and Ar^+.

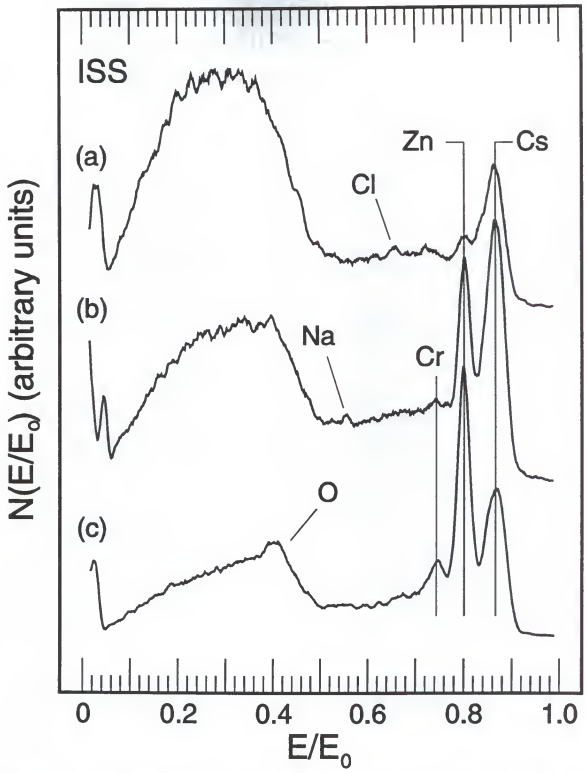

Figure 3-4. ISS spectra taken from the aged 3 wt.% Cs/Zn/Cr spinel catalyst after a) insertion into the UHV system; b) sputtering for 5 min with 1-keV He^+; c) sputtering for another 15 min with 1-keV 1:1 $He^+$and Ar^+.

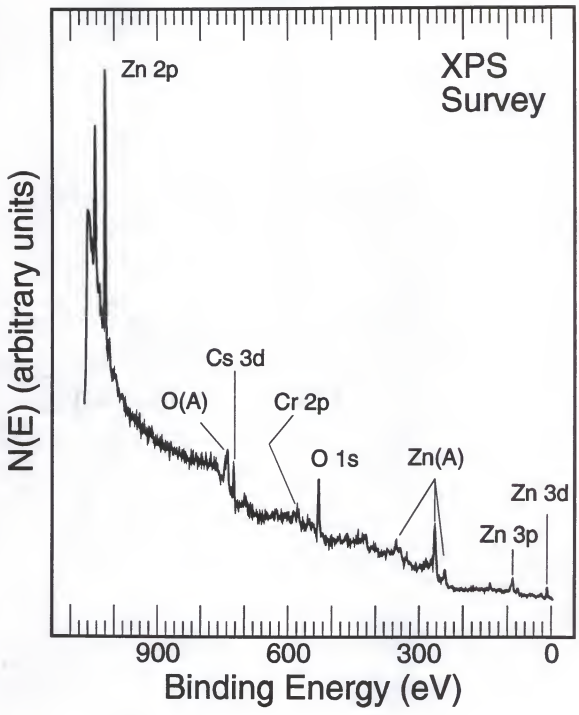

Figure 3-5. XPS survey spectrum taken from the nonreacted, nonpretreated, 3 wt.% Cs/Zn/Cr spinel catalyst.

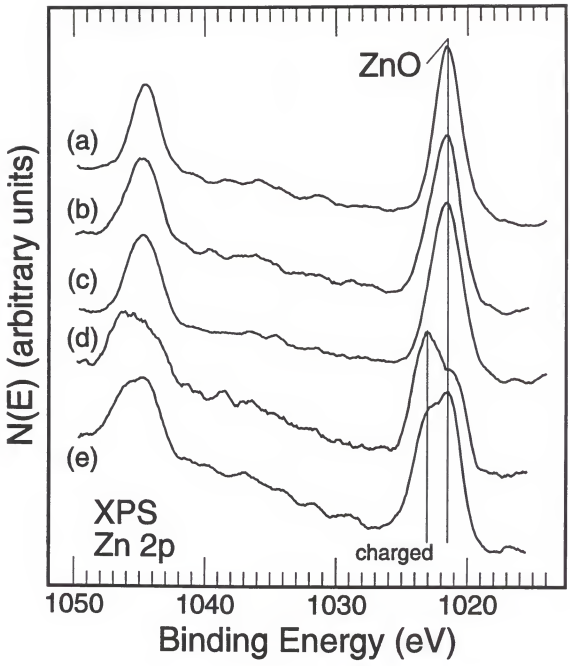

Figure 3-6. XPS Zn 2p spectra taken from the 3 wt.% Cs/Zn/Cr spinel catalyst after a) insertion into the UHV system; b) pretreating in 1 x 10^{-7} Torr of H_2 for 4 hrs at 250°C; c) sputtering for 5 min with 1-keV He^+ and 15 min with 1-keV 1:1 He^+ and Ar^+; d) the aged 3 wt.% Cs/Zn/Cr spinel catalyst; e) the aged catalyst after sputtering for 5 min with 1-keV He^+ and 15 min with 1-keV He^+ and Ar^+.

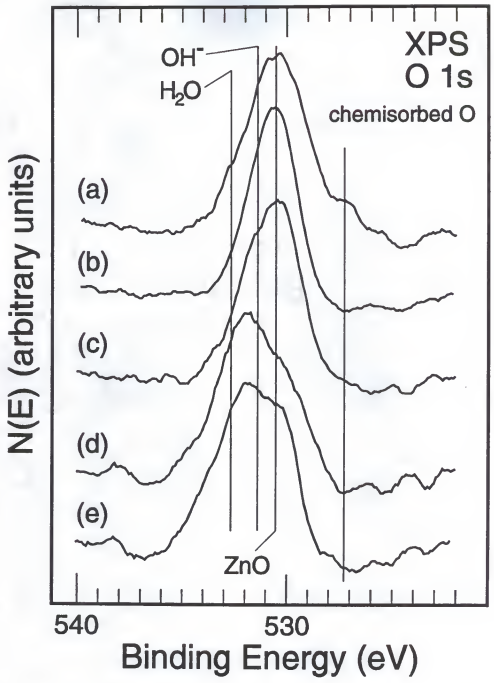

Figure 3-7. XPS O 1s spectra taken from the 3 wt.% Cs/Zn/Cr spinel catalyst after a) insertion into the UHV system; b) pretreating in 1 x 10^{-7} Torr of H_2 for 4 hrs at 250°C; c) sputtering for 5 min with 1-keV He^+ and 15 min with 1-keV 1:1 He^+ and Ar^+: d) the aged 3 wt.% Cs/Zn/Cr spinel catalyst; e) the aged catalyst after sputtering for 5 min with 1-keV He^+ and 15 min with 1-keV He^+ and Ar^+.

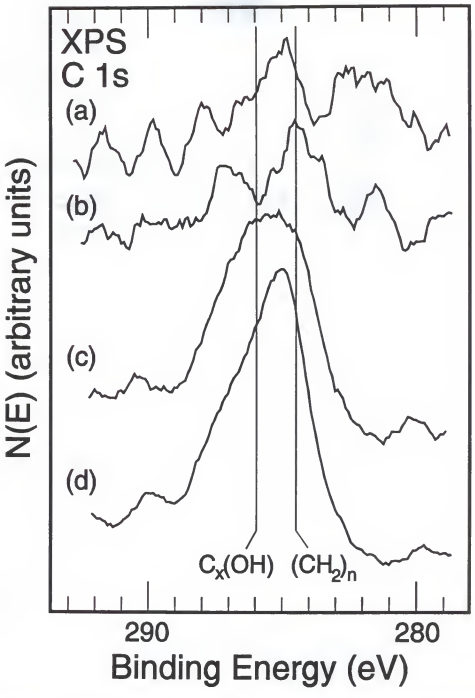

Figure 3-8. XPS C 1s spectra taken from the 3 wt.% Cs/Zn/Cr spinel catalyst after a) insertion into the UHV system; b) pretreating in 1 x 10^{-7} Torr of H_2 for 4 hrs at 250°C; c) sputtering for 5 min with 1-keV He^+ and 15 min with 1-keV 1:1 He^+ and Ar^+; d) the aged 3 wt.% Cs/Zn/Cr spinel catalyst.

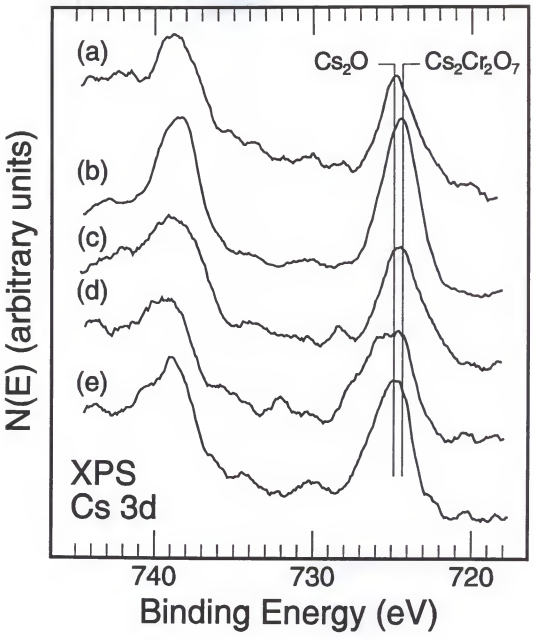

Figure 3-9. XPS Cs 3d spectra taken from the 3 wt.% Cs/Zn/Cr spinel catalyst after a) insertion into the UHV system; b) pretreating in 1 x 10^{-7} Torr of H_2 for 4 hrs at 250°C; c) sputtering for 5 min with 1-keV He^+ and 15 min with 1-keV 1:1 He^+ and Ar^+; d) the aged 3 wt.% Cs/Zn/Cr spinel catalyst; e) the aged catalyst after sputtering for 5 min with 1-keV He^+ and 15 min with 1-keV He^+ and Ar^+.

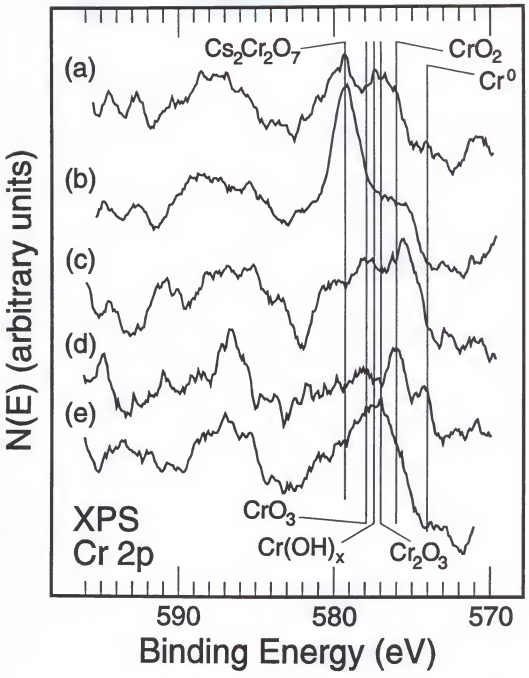

Figure 3-10. XPS Cr 2p spectra taken from the 3 wt.% Cs/Zn/Cr spinel catalyst after a) insertion into the UHV system; b) pretreating in 1 x 10^{-7} Torr of H_2 for 4 hrs at 250°C; c) sputtering for 5 min with 1-keV He^+ and 15 min with 1-keV 1:1 He^+ and Ar^+: d) the aged 3 wt.% Cs/Zn/Cr spinel catalyst; e) the aged catalyst after sputtering for 5 min with 1-keV He^+ and 15 min with 1-keV He^+ and Ar^+.

CHAPTER 4
STUDY OF A K-PROMOTED ZnO CATALYST FOR HAS

In the previous chapters, XPS data indicate that ZnO is the only phase present in the near-surface region after activating, reductive pretreatments have been performed. Based on this evidence ZnO may be the active catalytic phase for HAS. This hypothesis has been tested using a ZnO powder without and with K promotion as an HAS catalyst using a 1:1 H_2 and CO syngas feedstream.

Experimental

The ZnO powder was purchased from Aldrich Chemical Company. Using the incipient wetness method at a constant pH of 10, the powder samples were promoted by impregnation with 1, 3 and 5 wt.% K using potassium nitrate as the precursor. Each of these catalysts was then calcined in air at 325°C and reduced with a 5% hydrogen-in-nitrogen mixture for 4 hours at 300°C. Nonpromoted and promoted ZnO samples were tested for HAS catalytic activity using a 1:1 CO and H_2 syngas feed stream at a space velocity of 12,000 over 1 g of catalyst in a reactor which was described previously. Test measurements were taken while operating the reactor at temperatures of 400°C and 440°C and pressures of 1000 psi and 1500 psi. The catalysts were tested over a 5-day period to examine the activity as a function of time. During this period, the activity remained fairly constant.

Results and Discussion

Reaction Studies

A detailed listing of the product stream composition under the four different reactor conditions for the four different catalysts used is shown in table 4-1. Using the

nonpromoted sample results in relatively high production of methanol and hydrocarbon byproducts, but no higher alcohols are produced. The higher pressure and lower temperature operating condition result in increased methanol production. Contrary to results obtained from the Cs-promoted, commercial methanol-synthesis catalysts, at a reactor bed operating temperature of 440°C, the total alcohol rate and the selectivities to total alcohols are lower than when the reactor is operated at 400°C. This, however, is due to a greater methanol synthesis rate at the lower temperature. Very little or no isobutanol is produced at the lower operating temperature using any of the promoted ZnO catalysts examined. The HAS does occur more readily at the higher temperature. The higher pressure condition, 1500 psi, enhances the total alcohol flow rate as well. Only for the 5 wt.% K/ZnO catalyst does the 1000 psi operating pressure result in a greater isobutanol product flow rate. The higher pressure parameter also typically results in the larger syngas conversions as well. The lowest methanol-to-isobutanol mole ratios occur using the 440°C, 1000 psi operating parameters. The lowest ratio achieved is 2.3 using the 1 wt.% K/ZnO catalyst sample. The highest isobutanol product rate in most of the data presented is obtained at these operating conditions as well.

The effects of K-promotor concentration on the product stream composition was examined, and the rate of total alcohol production as a function of K loading at a reactor bed temperature of 440°C and a pressure of 1500 psi is shown in figure 4-1a. Using the nonpromoted catalyst results in an alcohol flow rate of almost 60 g/kg-hr, and the addition of K to the ZnO catalyst increases the total alcohol production rate. A maximum alcohol flow rate of 100 g/kg-hr is attained using the 3 wt.% K/ZnO sample while increasing the K loading to 5 wt.% decreases the total alcohol flow rate. The separate methanol and isobutanol product stream flow rates as a function of potassium loading are shown in figure 4-1b. Promoting the catalyst with 1 wt.% K increases the isobutanol flow rate from 0 to 38 g/kg-hr and yields a methanol-to-isobutanol mole ratio of 4.5. Increasing the K promotor concentration further, lowers the isobutanol product flow rate.

The highest methanol flow rate is achieved using the 3 wt.% K/ZnO catalyst which also corresponds to the greatest total alcohol flow rate discussed above. Further addition of K decreases the methanol product flow rate.

These results demonstrate that K-promoted ZnO is the active catalytic phase for HAS, but the synthesis of isobutanol over these ZnO catalysts is substantially lower than most values presented in the literature. These results, however, are not based on surface-area considerations but on catalyst weight. The BET surface area of the ZnO catalyst is approximately 18.5 m^2/gram while the BET surface areas of corresponding K-promoted, modified commercial catalysts discussed in the previous chapters are approximately 80 m^2/gram. Therefore, on a surface-area basis, the K-promoted ZnO catalyst would be superior in performance compared to the activities of other catalysts presented in the literature. This will be demonstrated in future studies by supporting the ZnO on high surface area supports. The Zn/Cr catalysts which have been investigated previously contain underlying Zn/Cr spinel structures which act as a high surface area support for the promoted ZnO at the surface. Both modified low-temperature and high-temperature methanol synthesis catalysts used for HAS contain Zn as one of the components. The data presented above suggest the other components, other than the alkali promotor, are not necessary for HAS. Campos-Martin et al. (40) and Forzatti et al. (49) have also examined Zn-containing catalysts for HAS. In both studies a ZnO phase was found using XRD. This is consistent with the assertion that ZnO is the active catalyst phase for HAS.

The selectivity to total alcohols as a function of promotor loading is shown in figure 4-2a. The addition of 1 wt.% K to the ZnO powder causes an increase in the alcohol product selectivity. Promoting the sample further results in even greater selectivities, but the rate of enhancement decreases. An alcohol selectivity of 87% is achieved using a 5 wt.% K/ZnO catalyst under the reaction conditions employed. As shown in figure 4-2b the increase in alcohol selectivity is due to a decrease in the hydrocarbon byproduct rate upon addition of the promotor. The data shown in figures 4-

2a and 4-2b are related directly and the figures are mirror images of each other. The product hydrocarbon rate using the nonpromoted catalyst is 100 g/kg-hr while that of the 5 wt.% K/ZnO catalyst is 6 g/kg-hr.

Characterization Studies

An XPS survey spectrum taken from the fresh, unreacted 1 wt.% K/ZnO catalyst is shown in figure 3a. Distinct Zn 2p, 3s, 3p and Auger features are apparent in this spectrum. An O 1s peak, an O Auger peak and a C 1s peak are present as well. The C consists of hydrocarbon and alcohol contamination which adsorbs during air exposure. After reducing the sample at 250°C for 4 hours in 1 x 10^{-7} Torr of H_2, the survey spectrum shown in figure 3b was obtained. The C ls peak is no longer evident, but K 2p features are now observable. The O 1s peak is decreased slightly in intensity indicating that the oxygen content of the near-surface region is reduced during the reductive treatment. This may be due partially to the elimination of O-containing carbon contamination. Similar XPS survey spectra were obtained from the other surfaces examined so they are not shown. The only differences are relatively small changes in peak intensities. The survey spectrum taken from the aged catalyst exhibits a larger O 1s feature indicating that O accumulates in the near-surface region during the reaction process. Furthermore, the survey spectrum taken from the aged catalyst sample does not contain the K 2p features but a C 1s peak is again evident. These changes are discussed in more detail in conjunction with the high-resolution spectra presented below.

The Zn 2p XPS spectrum taken from the fresh, nonpretreated sample is shown in figure 4a. The Zn $2p_{3/2}$ peak has a BE value of 1021.7 eV which corresponds to that of ZnO (58). No other features are observable in this spectrum. The Zn 2p peak shapes are quite symmetrical indicating that ZnO is the only chemial state of Zn present. A Zn 2p XPS spectrum taken from the reduced sample is shown in figure 4b. This spectrum is identical to that shown in figure 4a taken from the fresh sample. The XPS Zn 2p spectra

taken from the reduced sample after depth profiling, the aged sample and the aged sample after depth profiling are shown in figure 4c, 4d and 4e respectively, and no differences are observable between all the spectra shown. Similar results were obtained from characterization studies of the 3 wt.% K-promoted, Engelhard Zn/Cr spinel, HAS catalyst. Campos-Martin et al. used XPS to monitor the effects of Cs-promotion on the surface of a Cu/Zn/Cr HAS catalyst (40). They also observed no changes in the position or shape of the Zn $2p_{3/2}$ peak throughout the study which included Cs promotion and pretreatments. Therefore, the reductive pretreatment and the reaction process do not alter the chemical state of the Zn from ZnO over these HAS catalysts.

An XPS O 1s spectrum obtained from the fresh 1 wt.% K/ZnO sample is shown in figure 5a. The primary feature in this spectrum is due to the presence of hydroxyl groups in the near-surface region. A shoulder is evident at a BE value above 533 eV which indicates that adsorbed water is also present on the sample. The O 1s peak in this spectrum is broad and slightly asymmetric on the lower BE side where O in ZnO contributes to the O 1s signal. These data indicate that most of the oxygen in the near-surface region of the powder is not bound as ZnO, but as OH^- groups and adsorbed H_2O. Reduction of the sample at 250°C in 1 x 10^{-7} Torr of H_2 for 4 hours eliminates nearly all of the OH^- groups as shown in figure 5b. Some adsorbed water is still present, but most of the oxygen in the region probed by XPS is now bound as ZnO. The reductive treatment most likely removed the OH^- groups as water. After sputtering the catalyst with a 1-keV flux of a 1:1 Ar^+ and He^+ mixture for 15 minutes, the XPS O 1s spectrum shown in figure 5c was obtained. The sputtering process results in a decrease in the amount of adsorbed H_2O. The broadening of the O 1s peak on the higher BE side indicates that sputtering also leads to the exposure of OH^- groups which were originally beneath the probing depth of the XPS performed on the reduced catalyst. An XPS spectrum taken from the catalyst which was removed from the reactor after 5 days of use is shown in figure 5d. Most of the oxygen is bound as ZnO, however, a substantial

contribution to the signal due to OH^- groups is present as well. Sputtering the aged catalyst for 10 minutes with 1-keV He^+ and 15 minutes with 1-keV flux of a 1:1 He^+ and Ar^+ mixture removes some of the OH^- relative to ZnO in the near-surface region and does not expose any other chemical states of oxygen as shown in figure 5e.

An XPS spectrum of the C 1s and K 2p BE region of the fresh 1 wt.% K/ZnO powder is shown in figure 6a. Hydrocarbon and alcohol contaminants are present on the sample. No K 2p features are observable indicating that the fresh powder does not contain a significant quantity of K in the near-surface region. After the reductive pretreatment, the spectrum shown in figure 6b was taken. The reductive treatment causes an increase in the K concentration of the near-surface region as K 2p features are now apparent in the spectrum. Similar results were obtained after reductive pretreatments were performed on K- and Cs-promoted Engelhard Zn/Cr spinel catalysts. Identical high-temperature H_2 exposures increase the K or Cs concentrations at the surface of the spinels, but these promotors are bound with the Cr as chromate or dichromate species. The BE value of the K $2p_{3/2}$ in the present study is 294.3 eV, which is higher than the BE values of K_2CrO_4 and $K_2Cr_2O_7$. The K promotor on the ZnO catalyst must be in an oxidized state, but no species assignments can be made based on the K 2p values provided in the literature. In addition to increasing the K concentration in the near-surface region, the reductive treatment essentially eliminates all of the carbon contamination present on the fresh catalyst. Furthermore, no C is present in the subsurface region as shown in figure 6c which was obtained after sputtering the catalyst for 15 minutes. The K features have not changed in size although they do appear broader indicating that the sputtering process may alter the chemical state of a portion of the K or exposes other K species which are present beneath the near-surface region of the reduced catalyst. The corresponding spectrum taken from the aged catalyst is shown in figure 6d. The reaction process eliminates the near-surface K. Furthermore, a C 1s peak is present and its position indicates that an accumulation of alcohols occurs during the reaction

process. This is expected since methanol and isobutanol are the reaction products. Sputtering the aged catalyst reduces the amount of C as shown in figure 6e, and K is not apparent after sputtering. This indicates that K is not covered by other species during reaction so it must be removed from the catalyst surface by some mechanism as the reaction occurs.

As stated previously, ISS yields compositional information concerning the outermost atomic layer. An ISS spectrum taken from the fresh catalyst before pretreatment is shown in figure 7a. The outermost atomic layer consists of Zn, K, O and C. XPS data from this surface does not contain K features. This indicates that there is a small amount of K on the sample surface which is detected by ISS but not enough to produce an observable XPS peak. An ISS spectrum taken from the pretreated surface is shown in figure 7b. The large feature below an E/E_0 of 0.32 results from sample charging. The reductive treatment significantly increases the oxygen content of the outermost layer most likely through a chemically induced driving force. This increase in the oxygen content produces an insulating surface which results in sample charging and accounts for the observed feature. The Zn feature is barely observable, and the K-to-Zn ISS peak intensity is much greater than that of the fresh, nontreated sample. Therefore, the reductive treatment used to pretreat HAS catalysts produces an enrichment in K at the outermost atomic layer of the catalyst. This effect was observed in the XPS survey spectra discussed above and in the ISS data obtained from the K-promoted, Engelhard Zn/Cr spinel catalysts. This K may be present at the surface as K_2O. After sputtering the catalyst for 15 min with 1:1 He^+ and Ar^+, the ISS spectrum shown in figure 7c was taken. Much of the K and O have been sputtered away exposing more of the underlying ZnO.

The ISS spectrum taken from the aged catalyst shown in figure 8a indicates that the outermost surface layer of the catalyst becomes heavily contaminated with Na and Cl during reaction. As expected, Zn and O peaks are present as well as a small Al feature.

A small K feature also is observable as a shoulder on the high E/E_0 side of the Cl peak. After sputtering the aged catalyst for 5 min with 1-keV He^+, the ISS spectrum presented in figure 8b was taken. The Zn peak is increased in size relative to the Na and Cl contaminant features, and the K shoulder is reduced in size. Further sputtering results in almost complete removal of Na, Cl and Al as shown in figures 8c and 8d. The outermost surface layer of the aged catalyst which had been sputtered for 10 min with He^+ and 15 min with 1:1 He^+ and Ar^+ consists primarily of Zn and O (figure 8d) which is consistent with the XPS data presented above.

The reaction was run over the catalyst for a period of about five days. During this period, there was no significant variation in catalytic activity while the surface composition did vary quite significantly as shown by the ISS data in figures 7 and 8. Without an alkali ion present at the surface, ZnO is not active as a catalyst for HAS. This suggests that the active site may consist of a combination of Zn, O and alkali ions. During reaction, K was lost from the surface but replaced by subsurface Na. This explains why the activity did not decrease with the loss of K.

Summary

Nonpromoted and K-promoted ZnO powders were tested for higher alcohol synthesis using a 1:1 CO and H_2 syngas feedstream. Two pressure settings (1000 psi and 1500 psi) and two reactor bed temperature settings (400°C and 440°C) were used. The highest isobutanol rates are obtained at 440°C and 1500 psi using the 1 and 3 wt.% K-containing catalysts and at 440°C and 1000 psi using the 5 wt.% K-containing catalyst. No isobutanol is formed over the nonpromoted ZnO sample. The highest hydrocarbon byproduct rates occur at the 440°C and 1500 psi operating parameters. The addition of K to the ZnO decreases the hydrocarbon rate resulting in an increase in the alcohol selectivity. A maximum in the rate of isobutanol production as a function of K-

promotion is obtained using a 1 wt.% K/ZnO catalyst. At 440°C and 1500 psi, the use of this catalyst results in a methanol-to-isobutanol mole ratio of 4.5.

The XPS and ISS data were collected from the 1 wt.% K/ZnO powder. The near-surface region of the fresh sample consists primarily of ZnO and also contains hydrocarbon and alcohol contamination due to air exposure. The outermost layer does contain K according to the ISS data, but K is not observable in the XPS survey spectrum. Treating the sample in 1 x 10^{-7} Torr of H_2 at 250°C for 4 hours causes an enrichment of K in the near-surface region of the catalyst and results in an increase in oxygen at the outermost surface layer. Nearly all of the carbon contamination is eliminated by this pretreatment. The surface of the aged catalyst contains Na, Cl and Al contaminants. No K is present in the near-surface region according to the XPS data which indicates removal during reaction, but Na migrates to the surface from the subsurface region. The presence of alkali ions at the surface results in no significant decay during the one-week catalyst test period. This and the fact that ZnO without alkali ions at the surface is inactive catalytically suggest that the catalytic sites consist of Zn, O and alkali ions. Also, alcohols which are produced during reaction accumulate at the surface. The chemical state of Zn in the fresh, pretreated and aged samples is consistently ZnO.

Table 4-1. ZnO powder catalyst containing

	0% K				1% K				3% K				5% K			
P (psi) T (°C)	1000 400	1500 400	1500 440	1000 440	1000 400	1500 400	1500 440	1000 440	1000 400	1500 400	1500 440	1000 440	1000 400	1500 400	1500 440	1000 440
Selectivity to Total Alcohols (%)	57	68	23	15	84	91	70	72	95	98	82	76	96	98	87	88
Total Alcohol Rate (g/kg-hr)	74	164	59	23	72	157	85	41	79	156	100	46	56	95	68	25
Methanol Rate (g/kg-hr)	74	164	59	23	63	142	42	15	69	142	63	20	52	91	49	13
Ethanol Rate (g/kg-hr)	0	0	0	0	0	0	0	0	0	0	0	0	0	0	0	0
Isopropanol Rate (g/kg-hr)	0	0	0	0	0	0	0	0	0	0	2	1	2	0	0	0
n-Propanol Rate (g/kg-hr)	0	0	0	0	2	6	6	0	6	0	14	5	4	4	13	3
Isobutanol Rate (g/kg-hr)	0	0	0	0	7	8	38	26	4	14	22	20	0	0	6	9
MetOH/i-ButOH mole ratio	---	---	---	---	35	72	4.5	2.3	68	41	11	4.1	---	---	31	5.4
Hydrocarbon Rate (g/kg-hr)	28	38	100	67	7	7	23	10	2	2	12	9	1	1	6	2
Conversion (%)	9	10	11	8	7	8	8	7	9	10	11	9	7	7	7	7

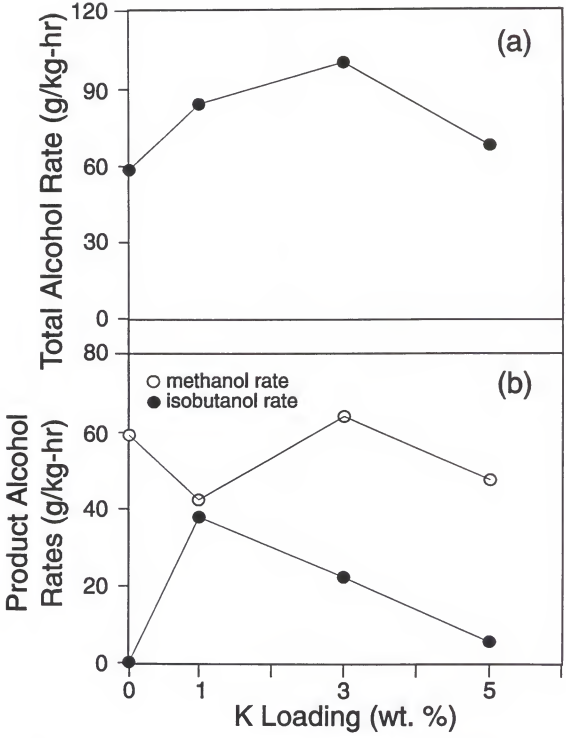

Figure 4-1. The effect of K loading when the reactor is operated at 440°C and 1500 psi on a) the total alcohol rate; b) the methanol and isobutanol rates of the product stream.

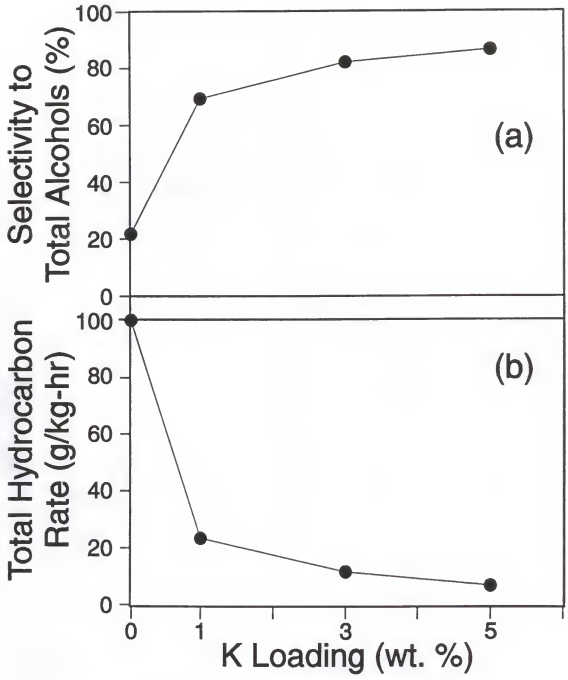

Figure 4-2. The effect of K loading when the reactor is operated at 440°C and 1500 psi on a) the selectivity to total alcohols; b) the total hydrocarbon rate.

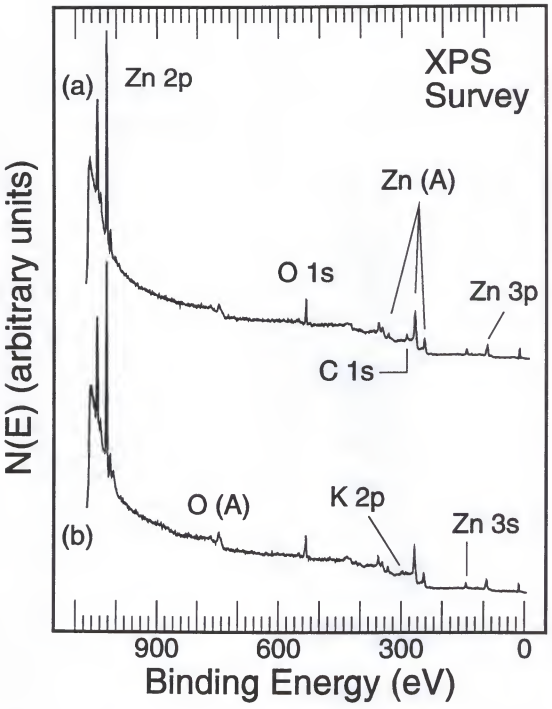

Figure 4-3. XPS survey spectrum taken from a fresh, unused 1 wt.% K/ZnO HAS catalyst after a) insertion into the UHV analysis chamber; b) exposure to 1 x 10^{-7}Torr of H_2 for 4 hrs at 250°C.

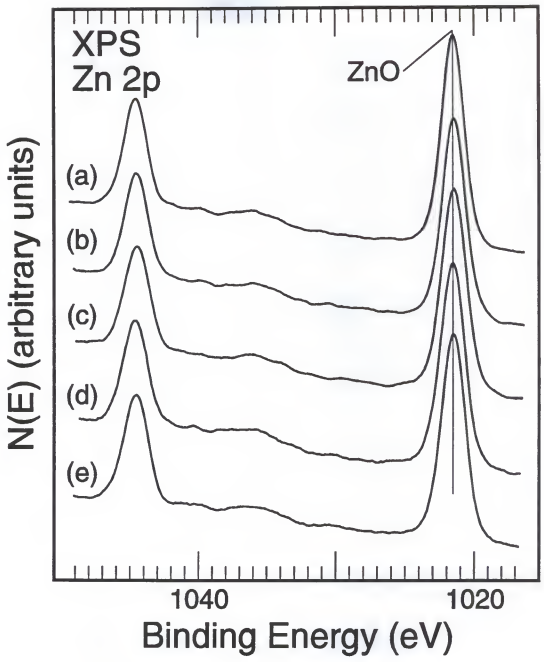

Figure 4-4. XPS Zn 2p spectra taken from a 1 wt.% K/ZnO HAS catalyst after a) insertion into the UHV system; b) pretreating in 1 x 10^{-7} Torr of H_2 for 4 hrs at 250°C; c) sputtering the sample with 1-keV He^+ and 15 min with 1-keV 1:1 He^+ and Ar^+; d) the aged 1 wt.% K/ZnO catalyst; e) the aged catalyst after sputtering for 5 min with 1-keV He^+ and 15 min with 1-keV He^+ and Ar^+.

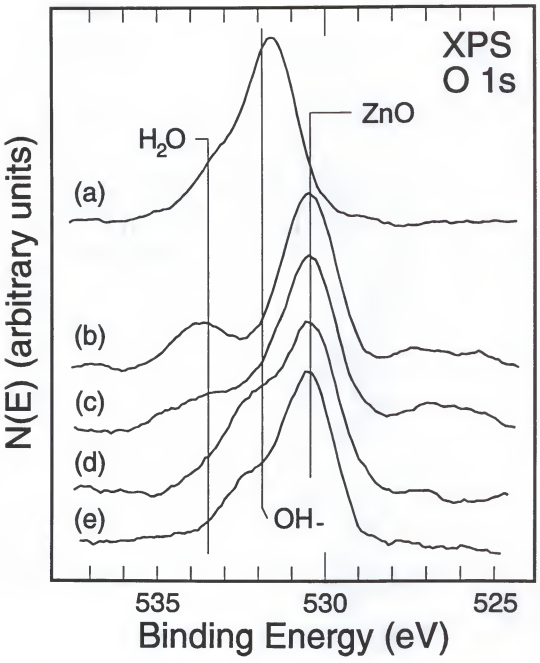

Figure 4-5. XPS O 1s spectra taken from the 1 wt.% K/ZnO HAS catalyst after a) insertion into the UHV system; b) pretreating in 1 x 10^{-7} Torr of H_2 for 4 hrs at 250°C; c) sputtering for 5 min with 1-keV He^+ and 15 min with 1-keV 1:1 He^+ and Ar^+: d) the aged 1 wt.% K/ZnO catalyst; e) the aged catalyst after sputtering for 5 min with 1-keV He^+ and 15 min with 1-keV He^+ and Ar^+.

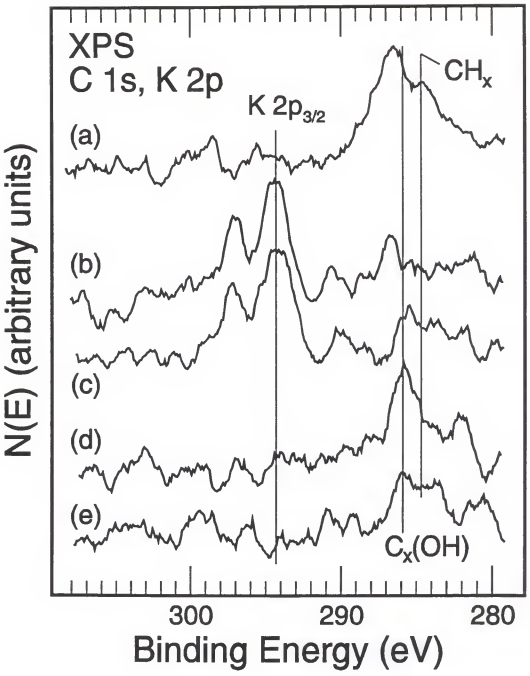

Figure 4-6. XPS C 1s and K 2p spectra taken from the 1 wt.% K/ZnO catalyst after a) insertion into the UHV system; b) pretreating in 1 x 10^{-7} Torr of H_2 for 4 hrs at 250°C; c) sputtering for 5 min with 1-keV He^+ and 15 min with 1-keV 1:1 He^+ and Ar^+; d) the aged 1 wt.% K/ZnO spinel catalyst; e) the aged catalyst after sputtering for 5 min with 1-keV He^+ and 15 min with 1-keV He^+ and Ar^+.

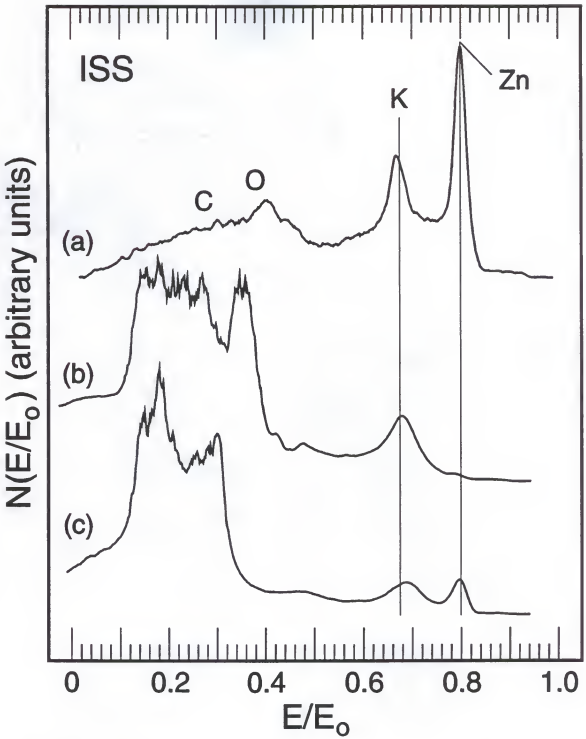

Figure 4-7. ISS spectra taken from the 1 wt.% K/ZnO HAS catalyst after a) insertion into the UHV system; b) pretreating in 1 x 10^{-7} Torr of H_2 for 4 hrs at 250°C; c) sputtering for 15 min with 1-keV 1:1 He^+ and Ar^+.

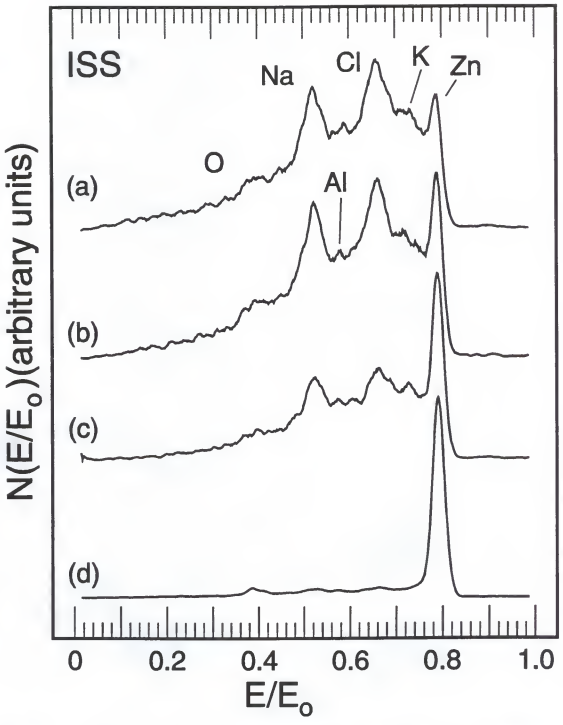

Figure 4-8. ISS spectra taken from the aged 1 wt.% K/ZnO HAS catalyst after a) insertion into the UHV system; b) sputtering for 5 min with 1-keV He^+; c) sputtering for another 5 min with 1-keV He^+; d) after an additional 15 min of sputtering using 1:1 He^+ and Ar^+.

REFERENCES

1. P.K. Frolich and D.S. Cryder, Industrial and Engineering Chemistry 22(1930)1051.

2. G.D. Graves, Industrial and Engineering Chemistry 23(1931)1381.

3. R.B. Anderson, B. Seligman, J.F. Schultz, R. Kelly and M.A. Elliot, Industrial and Engineering Chemistry 44(1952)391.

4. R.B. Anderson, B. Seligman, J.F. Schultz, R. Kelly and M.A. Elliot, Industrial and Engineering Chemistry 44(1952)2418.

5. D. Gall, E.J. Gibson and C.C. Hall, Journal of Applied Chemistry 2(1952)371.

6. J.F. Schultz, M. Abelson, L. Shaw and R.B. Anderson, Industrial and Engineering Chemistry 44(1952)397.

7. M. Pijolat and V. Perrichon, Applied Catalysis 13(1985)321.

8. K. Takeuchi, T. Matsuzaki, H. Arakawa and Y. Sugi, Applied Catalysis 18(1985)325.

9. K. Fujimoto and T. Oba, Applied Catalysis 13(1985)289.

10. A. Kiennemann, A. Barama, S. Boujana and M.M. Bettahar, Applied Catalysis A: General 99(1993)175.

11. M. Inoue, T. Miyake, S. Yonezawa, D. Mednahavyn, Y. Takegami and T. Inui, Journal of Molecular Catalysis 45(1988)111.

12. E.C. Alyea, D. He and J. Wang, Applied Catalysis A: General 104(1993)77.

13. P. Forzatti, E. Tronconi and I. Pasquon, Catalysis Review - Science and Engineering 33(1991)109.

14. X. Youchang, B.M. Naasz and G.A. Somorjai, Applied Catalysis 27(1986)233.

15. E.B. Pereira and G.A. Martin, Applied Catalysis A: General 103(1993)291.

16. S. Uchiyama, Y. Ohbayashi, T. Hayasaka and N. Kawata, Applied Catalysis 42(1988)143.

17. T. Tatsumi, A. Muramatsu and H. Tominaga, Applied Catalysis 34(1987)77.

18. M. Inoue, T. Miyake, Y. Takegami and T. Inui, Applied Catalysis 29(1987)618.

19. Ph. Courty, D. Durand, E. Freund and A. Sugier, Journal of Molecular Catalysis 17(1982)241.

20. K.M. Bailliard-Letournel, A.J. Gomez Cobo, C. Mirodatos, M. Primet and J.A. Dalmon, Catalysis Letters 2(1989)149.

21. X. Xiaoding, J.J. Schollen and D. Mausbeck, Applied Catalysis A: General 82(1992)91.

22. A. Kiennemann, C. Diagne, J.P. Hindermann, P. Chaumette and P. Courty, Applied Catalysis 53(1989)197.

23. P. Chaumette, Ph. Courty, A. Kiennemann, R. Kieffer, S. Boujana, G.A. Martin, J.A. Dalmon, P. Meriaudeau, C. Mirodatos, B. Holhein, D. Mausbeck, A.J. Hubert, A. Germain and A. Noels, Industrial and Engineering Chemistry Research 33(1994)1460.

24. J. Thivolle-Cazat, Applied Catalysis 24(1986)211.

25. A. Takeuchi and J.R. Katzer, Journal of Physical Chemistry 86(1982)2438.

26. A. Kiennemann, R. Breault, J.P. Hindermann and M. Laurin, Journal of the Chemical Society: Faraday Transactions I 83(1987)2119.

27. M. Ichikawa, T. Fukushima and K. Shikakura, Proceedings of the 8th International Congress of Catalysis (Berlin), VII (1984)69.

28. M. Ichikawa, Chem Tech (1982)674.

29. J.C. Lavalley, J. Saussey, J. Lamotte, R. Breault, J.P. Hindermann and A. Kiennemann, Journal of Physical Chemistry 94(1990)5941.

30. D. Yu-Hua, C. De-An and T. Khi-Rui, Applied Catalysis 35(1987)77.

31. G.C. Bond and D.G. Richards, Applied Catalysis 28(1986)303.

32. W.K. Lewis and P.K. Frolich, Industrial and Engineering Chemistry 20(1928)285.

33. J.F. Edwards and G.L. Schrader, Journal of Physical Chemistry 88(1984)5620.

34. J.F. Edwards and G.L. Schrader, Journal of Catalysis 94(1985)175.

35. G.A. Vedage, P.B. Himelfarb, G.W. Simmons and K. Klier, American Chemical Society Symposium Series 279(1985)295.

36. J. Nunan, K. Klier, C.-W. Young, P.B. Himelfarb and R.D. Herman, Journal of the Chemical Society, Chemistry Communications 3(1986)193.

37. J.G. Nunan, C.E. Bogdan, K. Klier, K.J. Smith, C.W. Young and R.G. Herman, Journal of Catalysis 113(1988)410.

38. J.G. Nunan, C.E. Bogdan, K. Klier, K.J. Smith, C.W. Young and R.G. Herman, Journal of Catalysis 116(1989)195.

39. J.G. Nunan, R.G. Herman and K. Klier, Journal of Catalysis 116(1989)222.

40. J.M. Campos-Martin, J.L.G. Fierro, A. Guerrero-Ruiz, R.G. Herman and K. Klier, Journal of Catalysis 163(1996)418.

41. A. Beretta, Q. Sun, R.G. Herman and K. Klier, Industrial and Engineering Chemistry Research 35(1996)1534.

42. K.J. Smith and R.B. Anderson, Canadian Journal of Chemical Engineering 61(1983)40.

43. I. Boz, M. Sahibzada and I.S. Metcalfe, Industrial and Engineering Chemistry Research 33(1994)2021.

44. E.M. Calverley and K.J. Smith, Journal of Catalysis 130(1991)616.

45. E.M. Calverley and K.J. Smith, Industrial and Engineering Chemistry Research 31(1992)792.

46. A.B. Stiles, F. Chen, J.B. Harrison, X. Hu, D.A. Storm and H.X. Yang, Industrial and Engineering Chemistry Research 30(1991)811.

47. A. Kiennemann, H. Idriss, R. Kieffer, P. Chaumette and D. Durand, Industrial and Engineering Chemistry Research 30(1991)1130.

48. B.B. Breman, A.C.C.M. Beenackers and E. Oesterholt, Chemical Engineering Science 49(1994)4409.

49. P. Forzatti, C. Cristiani, N. Ferlazzo, L. Lietti, E. Tronconi, P.L. Villa and I. Pasquon, Journal of Catalysis 111(1988)120.

50. C. Cristiani, P. Forzatti and M. Bellotto, Journal of the Chemical Society, Faraday Transactions 1 85(1989)895.

51. E. Tronconi, L. Lietti, P. Forzatti and I. Pasquon, Applied Catalysis 47(1989)317.

52. G.V. Itina, A.A. Davydov, M.A. Osipova and L.N. Kurina, Reaction Kinetics and Catalysis Letters 45(1991)243.

53. W. Keim and W. Falter, Catalysis Letters 3(1989)59.

54. F. Simard, U.A. Sedran, J. Sepulveda, N.S. Figoli and H.I. Lasa, Applied Catalysis A: General 125(1995)81.

55. E. Tronconi, P. Forzatti and I. Pasquon, Journal of Catalysis 124(1990)376.

56. E. Tronconi, N. Ferlazzo, P. Forzatti and I. Pasquon, Industrial and Engineering Chemistry Research 26(1987)2122.

57. L. Lietti, E. Tronconi and P. Forzatti, Journal of Catalysis 135(1992)400.

58. C.D. Wagner, W.M. Riggs, L.E. Davis, J.F. Moulder and G.E. Muilenberg, Handbook of X-ray Photoelectron Spectroscopy, Perkin-Elmer, Eden Prairie, Minnesota, 1979.

59. R.E. Gilbert, D.F. Cox and G.B. Hoflund, Review of Scientific Instruments 53(1982)1281.

60. M.R. Davidson, G.B. Hoflund and R.A. Outlaw, Journal of Vacuum Science and Technology A 9(1991)1344.

61. T.L. Barr and J. Hackenberg, Applied Surface Science 10(1982)523.

62. C. Baltistoni, J.L. Dormann, D. Fiorani, E. Paparazzo and S. Viticoli, Solid State Communications 39(1981)581.

63. J.F. Weaver and G.B. Hoflund, Journal of Physical Chemistry 98(1994)8519.

64. V.I. Nefedov, Y.V. Salyn, P.M. Solozhenkin and G.Y. Putatov, Surface and Interface Analysis 2(1980)171.

65. G.C. Allen, M.T. Curtis, A.J. Hooper and P.M. Tucker, Journal of the Chemical Society Dalton Transactions 9(1973)1677.

66. T. Tsutsumi, I. Ikemoto, T. Namikawa and H. Kuroda, Bulletin of the Chemical Society of Japan 54(1981)913.

67. I. Ikemoto, K. Ishii, S. Kinoshita, H. Kuroda, M.A.A. Franco and J.M. Thomas, Journal of Solid State Chemistry 17(1976).

68. F.M. Capece, V. DiCastro, C. Furlani, G. Mattogno, C. Fragale, M. Gargano and M. Rossi, Journal of Electron Spectroscopy and Related Phenomena 27(1982)119.

69. S.J. Yang and C.W. Bates, Applied Physics Letters 36(1980)675.

70. G.C. Allen and P.M. Tucker, Inorg Chim Acta 16(1976)41.

BIOGRAPHICAL SKETCH

William S. Epling, Jr., was born on December 30, 1970, in Pensacola, Florida, to Ann Elizabeth Epling and William Stelbourne Epling, Sr. As a son of an officer in the United States Navy, he was able to travel to Alaska, Okinawa, Philippines, Puerto Rico and finally Virginia. William began his college education at Virginia Tech in 1988 and graduated in chemical engineering in 1992. At that time, he chose to continue his education as a graduate student in chemical engineering at the University of Florida. William currently performs research in surface science and catalyst development.

I certify that I have read this study and that in my opinion it conforms to acceptable standards of scholarly presentation and is fully adequate, in scope and quality, as a dissertation for the degree of Doctor of Philosophy.

Gar B. Hoflund, Chairman
Professor of Chemical Engineering

I certify that I have read this study and that in my opinion it conforms to acceptable standards of scholarly presentation and is fully adequate, in scope and quality, as a dissertation for the degree of Doctor of Philosophy.

Dinesh O. Shah
Professor of Chemical Engineering

I certify that I have read this study and that in my opinion it conforms to acceptable standards of scholarly presentation and is fully adequate, in scope and quality, as a dissertation for the degree of Doctor of Philosophy.

Seymour S. Block
Professor Emeritus of Chemical Engineering

I certify that I have read this study and that in my opinion it conforms to acceptable standards of scholarly presentation and is fully adequate, in scope and quality, as a dissertation for the degree of Doctor of Philosophy.

Lucy Elizabeth Seiberling
Associate Professor of Physics

I certify that I have read this study and that in my opinion it conforms to acceptable standards of scholarly presentation and is fully adequate, in scope and quality, as a dissertation for the degree of Doctor of Philosophy.

Vaneica Y. Young
Associate Professor of
Chemistry

This dissertation was submitted to the Graduate Faculty of the College of Engineering and to the Graduate School and was accepted as partial fulfillment of the requirements for the degree of Doctor of Philosophy.

August 1997

Winfred M. Phillips
Dean, College of Engineering

Karen A. Holbrook
Dean, Graduate School